Available online at www.sciencedirect.com
SCIENCE DIRECT®
Coordination Chemistry Reviews 248 (2004) 725–756
COORDINATION CHEMISTRY REVIEWS
www.elsevier.com/locate/ccr

Review

Nonlinear optical properties of transition metal acetylides and their derivatives☆

Clem E. Powell, Mark G. Humphrey*

Department of Chemistry, Australian National University, Canberra, ACT 0200, Australia

Received 30 September 2003; accepted 1 March 2004

Contents

Abstract

The nonlinear optical (NLO) properties of metal acetylide and vinylidene complexes are summarized, and molecular structure–NLO property trends are developed. The origin of NLO effects in molecules is presented, and the advantages and shortcomings of experimental

☆ Contribution to the special issue "Modern Aspects of Organometallic Chemistry".

* Corresponding author. Tel.: +61-2-6125-2927; fax: +61-2-6125-0760.
E-mail address: mark.humphrey@anu.edu.au (M.G. Humphrey).

0010-8545/$ – see front matter
doi:10.1016/j.ccr.2004.03.009

procedures that have been used to measure optical nonlinearities for these complexes are discussed. Attempts to "switch" optical nonlinearities of acetylide or vinylidene complexes are summarized.

Keywords: Acetylide complexes; Alkynyl complexes; Vinylidene complexes; Nonlinear optics; Hyperpolarizabilities; Quadratic nonlinearities; Cubic nonlinearities

1. Introduction

While an overview of the theory of nonlinear optics and experimental procedures to measure nonlinear optical (NLO) responses is a necessary prerequisite to the survey of NLO properties of acetylide and vinylidene complexes that follows, excellent reviews of the field of nonlinear optics, and of the NLO properties of organic [1–6] and, particularly, organometallic molecules [7–12] are available elsewhere, so the present introduction to the field is abbreviated. When light interacts with materials possessing NLO properties the incident light can be changed and new electromagnetic field components produced (e.g. with differing phase, frequency, amplitude, polarization, path, etc.). NLO materials have potential applications in optical signal processing, switching and frequency generation (making use of processes such as harmonic generation, frequency mixing, and optical parametric oscillation), and may also contribute to optical data storage, optical communication, and image processing.

Current NLO materials are mostly inorganic salts ($LiNbO_3$ and KH_2PO_4 (KDP) are used for frequency mixing and electrooptic modulation) or glasses such as silica (for applications involving third-order nonlinear processes). In inorganic salts the purely electronic NLO effects are often accompanied by those arising from lattice distortions, with response times in the order of nanoseconds; the latter can be useful for relatively slow NLO processes (e.g. the electrooptic effect), but not for frequency conversions which require a purely electronic NLO response. Inorganic salts possess a large transparency range, are robust, are available as large single crystals, and suffer very low optical losses. The frequency doubling of lasers and optical parametric amplification require synchronization of the phases of the interacting optical fields (phase matching) which is not easy to satisfy, severely limiting the application of some materials. Semiconductors possess NLO effects originating from saturable absorption [13]. Their third-order NLO responses are amongst the largest known [14], but NLO processes based on such resonant interactions may be relatively slow.

The limitations identified above spurred investigation of organic and, more recently, organometallic compounds. Many organic molecules have been examined for their NLO responses [1–6,15–22], the main source of which is usually the electronic nonlinearities. Organic materials can possess a number of advantages, including a higher optical damage threshold than inorganic crystals, ease of synthesis and fabrication, structural diversity and architectural flexibility (permitting molecular design and engineering), and facile use in thin films for which electric field poling can introduce the asymmetry needed for the appearance of second-order NLO effects. Organics have several disadvantages: low energy transitions in the UV-Vis region enhance the NLO efficiency, but result in a trade-off between nonlinear efficiency and optical transparency, they may have low thermal stability and (in poled guest–host systems) they may undergo a facile relaxation to random orientation.

Organometallic complexes are similar to organic molecules in that they can possess large NLO responses, fast response times, ease of fabrication and integration into composites. However, they possess the advantage of much greater design flexibility, e.g. by variation in metal, oxidation state, ligand environment and geometry, and can be strong oxidizing or reducing agents. The metal center may be an extremely strong donor or acceptor, a requirement for electron asymmetry and hence second-order nonlinearity. Unusual and/or unstable organic fragments (e.g. vinylidenes) may be stabilized on metals, allowing the NLO properties of these species to be assessed. The NLO properties of organometallic compounds have been reviewed previously together with those of some related coordination complexes [8,12,23–26].

Metal acetylide complexes were first reported in the 1950s [27], and have recently attracted significant interest because of possible materials applications [28,29]. This review focuses on the NLO properties of metal acetylide (alkynyl) complexes and their derivatives; they form an important subset of organometallic complexes for nonlinear optics, in that they can have high optical nonlinearities and have recently been shown to undergo facile NLO switching.

2. Theory and processes

2.1. Theory of nonlinear optics

Optical nonlinearities can be explained by considering the interaction of strong electric fields with matter. A local electric field $\boldsymbol{E}_{\mathrm{loc}}$ acting on a molecule will distort its electron density distribution $\rho(\boldsymbol{r})$, a result that can be described in terms of changes in the electron distribution moments. The first electron distribution moment, the dipole moment $\boldsymbol{\mu}$, is the most important moment from the perspective of optical properties. Changes in the dipole moment induced by a weak field are linear with the magnitude of the field. This is not the case when $\boldsymbol{E}_{\mathrm{loc}}$ is comparable in strength to the internal electric fields within the molecule, at which point the

distortion and the induced dipole moment should be treated as nonlinear functions of the field strength, usually being presented as a power series:

$$\boldsymbol{\mu} = \boldsymbol{\mu}_0 + \alpha \boldsymbol{E}_{\mathrm{loc}} + \beta \boldsymbol{E}_{\mathrm{loc}} \boldsymbol{E}_{\mathrm{loc}} + \gamma \boldsymbol{E}_{\mathrm{loc}} \boldsymbol{E}_{\mathrm{loc}} \boldsymbol{E}_{\mathrm{loc}} + \cdots \quad (1)$$

The tensors α, β and γ defined by the above equation are the linear polarizability, the second-order or quadratic hyperpolarizability (the first hyperpolarizability) and the third-order or cubic hyperpolarizability (the second hyperpolarizability), respectively. Both $\boldsymbol{\mu}$ and $\boldsymbol{E}_{\mathrm{loc}}$ are vectors, so the relation between the three Cartesian components of $\boldsymbol{\mu}$ and the three Cartesian components of $\boldsymbol{E}_{\mathrm{loc}}$ needs nine proportionality factors, and hence α is a second-rank tensor (or a 3×3 matrix). Analogously, β is a third-rank tensor (or a $3 \times 3 \times 3$ matrix) and γ is a fourth-rank tensor (or a $3 \times 3 \times 3 \times 3$ matrix). Fortunately, many of the tensor components of α, β, and γ are equivalent by various symmetry rules or equal to zero. The most straightforward simplification comes from permutation symmetry [30]. Additional simplification comes from polarizabilities being invariant with respect to all point group symmetry operations, this rule being especially important when considering β: all the components of β must vanish in centrosymmetric point groups.

The electric field of a light wave can be expressed as:

$$\boldsymbol{E}(t) = \boldsymbol{E}_0 \cos(\omega t) = \tfrac{1}{2}\boldsymbol{E}_0[\exp(\mathrm{i}\omega t) + \exp(-\mathrm{i}\omega t)]$$

so Eq. (1) can be written as:

$$\begin{aligned}\boldsymbol{\mu}(t) &= \boldsymbol{\mu}_0 + \alpha \boldsymbol{E}_0 \cos(\omega t) + \beta \boldsymbol{E}_0^2 \cos^2(\omega t) \\ &\quad + \gamma \boldsymbol{E}_0^3 \cos^3(\omega t) + \cdots, \\ \boldsymbol{\mu}(t) &= \boldsymbol{\mu}_0 + \tfrac{1}{2}\alpha \boldsymbol{E}_0 \exp(\mathrm{i}\omega t) + \tfrac{1}{2}\beta \boldsymbol{E}_0^2 + \tfrac{1}{4}\beta \boldsymbol{E}_0^2 \exp(2\mathrm{i}\omega t) \\ &\quad + \tfrac{3}{8}\gamma \boldsymbol{E}_0^3 \exp(\mathrm{i}\omega t) + \tfrac{1}{8}\gamma \boldsymbol{E}_0^3 \exp(3\mathrm{i}\omega t) + \mathrm{cc} + \cdots\end{aligned} \quad (2)$$

where cc stands for complex conjugate terms. It is readily apparent from the above expansions in terms of exponential factors or, equivalently, trigonometric relations such as $\cos^2(\omega t) = 1/2 + 1/2\cos(2\omega t)$ that the effect of the nonlinear terms in the dipole moment expansion has been to introduce contributions at different frequencies: the second-order (β) term has introduced a time-independent (dc) contribution as well as a term oscillating at the frequency of 2ω (the second-harmonic generation component). The quadratic term also provides a frequency mixing phenomenon if the input field is a sum of two components with different frequencies. It is also readily apparent that a constant (dc) field may influence an oscillating field if the two are combined in a medium containing second-order nonlinear molecules [this is known as the linear electrooptic (Pockels) effect]. The cubic term in Eq. (1) leads to several nonlinear optical effects, one being oscillation of the induced dipoles at 3ω (third-harmonic generation).

Eq. (1) is, strictly speaking, not suitable for optical fields, which are rapidly varying in time. For linear polarization, the oscillation of the induced dipole moment may be damped (by material resonances) and thereby phase shifted with respect to the oscillation of the external electric field. This is usually expressed by considering the relationship between the Fourier components of the induced effect (oscillation of the induced dipole) and the stimulus (the electric field), with the damping and phase shift conveniently expressed by treating the terms involved as complex. The linear polarizability can then be written as:

$$\Delta\mu^{(1)}(\omega) = \alpha(\omega)E(\omega)$$

where $\alpha(\omega)$ is complex, $E(\omega)$ is the Fourier amplitude of the field at frequency ω and $\Delta\mu^{(1)}(\omega)$ is the linear component of the oscillation of the dipole at the same frequency. The real part of α changes rapidly and the imaginary part of α increases in value near to the resonance frequencies of the molecule. Similarly, frequency dependent hyperpolarizabilities can be defined as complex quantities by considering the relations between the nonlinear (quadratic and cubic) components of the induced dipole moment oscillations at particular frequencies, a complication being that more than a single field frequency is usually involved. The usual notation is:

$$\Delta\mu^{(2)}(\omega_3) = \beta(-\omega_3; \omega_1, \omega_2)E(\omega_1)E(\omega_2)$$

and

$$\Delta\mu^{(3)}(\omega_4) = \gamma(-\omega_4; \omega_1, \omega_2, \omega_3)E(\omega_1)E(\omega_2)E(\omega_3)$$

for the quadratic and cubic NLO effects, respectively. The first frequency in the brackets describing the frequency dependence of the hyperpolarizability corresponds to the output frequency, the remaining frequencies being those of the input fields. Positive and negative signs of the frequencies can occur, depending on the type of interaction: for example, the β responsible for second-harmonic generation (SHG) is represented as $\beta(-2\omega; \omega, \omega)$ whereas β for optical rectification is written as $\beta(0; -\omega, \omega)$. Resonant behavior of the hyperpolarizabilities (a rapidly changing real part and enhanced imaginary part) is expected not only when one of the frequencies in $\beta(-\omega_3; \omega_1, \omega_2)$ or $\gamma(-\omega_4; \omega_1, \omega_2, \omega_3)$ approaches a resonance but also for some combination of the input frequencies being close to a resonance.

Description of macroscopic NLO phenomena is analogous to the microscopic approach presented above. The macroscopic quantities of interest are the susceptibilities of various orders defined by:

$$\boldsymbol{P} = \chi^{(1)}\boldsymbol{E} + \chi^{(2)}\boldsymbol{E}^2 + \chi^{(3)}\boldsymbol{E}^3 + \cdots$$

$\chi^{(\mathrm{i})}$ are tensors of the same ranks as their molecular analogues and, similarly, the equation relating the polarization to the macroscopic optical field is rewritten in terms of the Fourier components of the polarization and of the input fields. The macroscopic NLO properties are treated as the sum of molecular contributions, allowing for orientation of the molecules and for differences between the local

field and the macroscopic electrical field. Tensor properties are usually transformed from one coordinate system to another using matrices of orientational cosines. Following this approach, the second-order susceptibility $\chi^{(2)}$ of a crystal composed of organic molecules with second-order hyperpolarizability β is equal to [31]:

$$\chi^{(2)}_{IJK}(-\omega_3;\omega_1,\omega_2) = L_I(\omega_3)L_J(\omega_1)L_K(\omega_2)\sum_{t=1}^{p}N_t b^t_{IJK}(-\omega_3;\omega_1,\omega_2)$$

where the L factors are the local field factors (usually approximated by the Lorenz–Lorentz expression $L = (n^2+2)/3$, where n is the refractive index), and for which:

$$b^t_{IJK}(-\omega_3;\omega_1,\omega_2) = \frac{1}{N_g}\sum_{ijk}\sum_{s=1}^{N_g}\cos\theta^{(s)}_{Ii_t}\cos\theta^{(s)}_{Jj_t}\cos\theta^{(s)}_{Kk_t}\beta_{ijk}(-\omega_3;\omega_1,\omega_2)$$

where *ijk* denotes the Cartesian coordinates of a molecule, *IJK* those of a crystal (a unit cell), N_t is the number of molecules in a unit volume occupying each particular inequivalent site in the unit cell, p is the number of inequivalent positions of a molecule in a unit cell and N_g is the number of equivalent positions in a unit cell. The directional cosines are used to transform each of the molecular β components to those of the new coordinate system (b_{IJK}) and the contributions are summed.

Owing to statistical orientation of molecules, orientation averaging can be performed; for fourth-rank tensors; this leads to substantial simplification. From symmetry considerations, the $\chi^{(3)}$ tensor for an isotropic medium can only have two independent components, namely $\chi^{(3)}_{1111}$ and $\chi^{(3)}_{1122}$. The component $\chi^{(3)}_{1111}$ can be related to components of the molecular hyperpolarizability tensor as follows:

$$\chi^{(3)}_{1111}(-\omega_4;\omega_1,\omega_2,\omega_3) = L_{\omega_1}L_{\omega_2}L_{\omega_3}L_{\omega_4}N\langle\gamma(-\omega_4;\omega_1,\omega_2,\omega_3)\rangle$$

where L_{ω_i} is the local field factor at frequency ω_i (usually approximated by the Lorenz–Lorentz expression $L_\omega = (n^2_\omega+2)/3$) and

$$\langle\gamma\rangle = \tfrac{1}{5}(\gamma_{1111}+\gamma_{2222}+\gamma_{3333}+2\gamma_{1122}+2\gamma_{1133}+2\gamma_{2233})$$

The simplest case is that of an isotropic medium containing molecules with a single dominant component of γ, say γ_{1111} (a realistic approximation for linear π-conjugated molecules, for which the hyperpolarizability component along the molecular axis is likely to be dominant); $\langle\gamma\rangle = 1/5(\gamma_{1111})$ is then a reasonable approximation.

The two common unit systems employed for the description of nonlinear optical properties are the SI (or MKS) and Gaussian (or cgs) systems. We have discussed conversions between these systems of units elsewhere [10,11]. The Gaussian system (in which properties are described in terms of esu) has been used in almost all reports of metal acetylide or vinylidene complexes thus far.

2.2. Nonlinear optical processes

The major use of second-order nonlinearities is for a variety of frequency mixing schemes. Among the possible processes, there are several which have specific technological applications and are therefore of significant interest: (i) second-harmonic generation, i.e. the $\omega+\omega\rightarrow 2\omega$ mixing process which doubles the energy of photons (e.g. to convert infrared into visible light); (ii) the linear electrooptic (Pockels) effect, i.e. the $\omega+0\rightarrow\omega$ process which is often used to modulate the phase or amplitude of a light wave (to make it carry information); and (iii) parametric generation, i.e. the $\omega\rightarrow\omega_1+\omega_2$ process which involves splitting an energetic photon into a sum of two less energetic ones (a popular way of generating laser beams at tunable wavelengths).

There are many possible third-order nonlinear processes, some of which are important as valuable tools for nonlinear spectroscopy, while others have technological significance. The presence of $\chi^{(3)}$ in any substance (even air) means that all materials exhibit third-harmonic generation of laser frequencies. The direct process of third-harmonic generation is, however, not usually exploited for generation of short wavelength laser beams, a cascade of two second-order mixing processes ($\omega+\omega\rightarrow 2\omega$ and $2\omega+\omega\rightarrow 3\omega$) being preferred for generation of 3ω from ω (one reason for this is that phase matching is virtually impossible to obtain for third-harmonic generation). From the technological point of view, the most interesting applications of $\chi^{(3)}$ are those which correspond to all-optical interactions of light beams. For interacting fields of the same frequency (the degenerate case), the frequency mixing scheme is $\omega-\omega+\omega\rightarrow\omega$, which means that the interaction of three fields of the same frequency generates a fourth field of the same frequency.

Optical power limiting has attracted considerable interest with applications such as the protection of sensors from damage resulting from exposure to high energy laser pulses. In principle, the direct two-photon absorption process is suitable for optical limiting, but practical estimates show that power limiting properties of existing materials (even those with the largest two-photon absorption coefficients such as ruthenium acetylide dendrimers—see later discussion) are insufficient for the most important applications, namely the protection of sensors from laser pulses of duration of the order of nanoseconds.

3. Experimental techniques

A large number of techniques have been employed to measure quadratic and cubic nonlinearities of organic molecules, excellent descriptions of which can be found elsewhere [32]. The discussion that follows is restricted to techniques utilized with metal acetylide and vinylidene complexes.

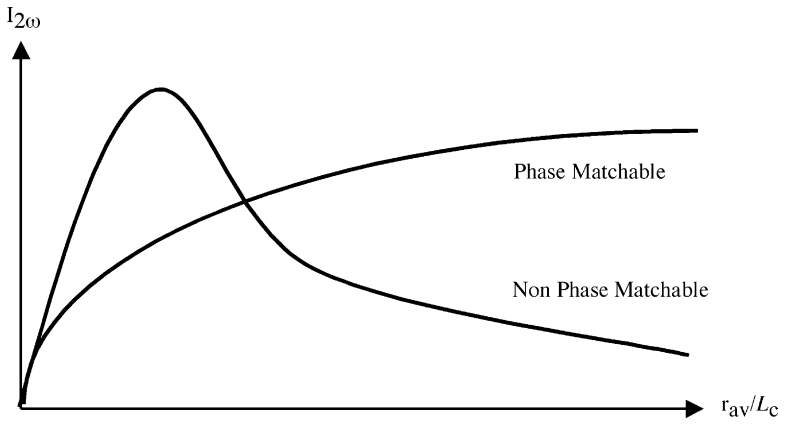

Fig. 1. Particle size dependence of the second-harmonic intensity. Reprinted by permission of the American Institute of Physics from S.K. Kurtz and T.T. Perry, J. Appl. Phys. 39 (1968) 3798.

3.1. Kurtz powder technique

In this procedure a laser beam is directed onto a powder sample and the emitted second-harmonic light is collected, filtered, detected and compared with a standard (usually urea). As the magnitude of the response depends on particle size, samples are commonly sieved to ensure a narrow particle size range. Materials can be classed as phase matchable or non-phase matchable (Fig. 1). For the latter, second-harmonic generation is effective over distances smaller than the coherence length (the coherence length L_c for a second-harmonic process is given by $L_c = [\lambda_\omega/4(n_{2\omega} - n_\omega)]$ for fundamental wavelength λ_ω and the refractive indices of the material at the fundamental n_ω and second-harmonic $n_{2\omega}$). When the light path is smaller than the coherence length the second-harmonic intensity increases with the square of the interaction distance. However, when the crystal sizes are similar to the coherence length, there is no further increase of second-harmonic intensity with the propagation distance and the signal actually decreases, due to the number of crystals sampled decreasing. In contrast, there is a direction of propagation in phase matchable materials for which the second harmonic intensity increases quadratically without a limit. The SHG intensity does not decrease because the decrease in the number of crystallites as they become bigger is compensated by the contribution from phase-matched interactions. Fig. 1 demonstrates the differing behavior of non-phase matched and phase-matched materials.

Because the light intensities measured in the powder technique depend on several factors, results from Kurtz SHG studies should not be considered as quantitative. The magnitude of the tensor components of the molecular hyperpolarizability β is only one of these factors. A critical issue is the molecular packing in the unit cell of the crystal. The unit cell hyperpolarizability tensor components are all identically equal to zero in a centrosymmetric arrangement. In noncentrosymmetric arrangements, substantial differences in the nonlinear coefficients may result from packing nonlinear molecules in different ways. Unit cell hyperpolarizability is transformed into macroscopic second-order susceptibility with the contribution of local field factors; this can modify the properties also. SHG efficiency is critically dependent on the coherence lengths, which depend in turn on crystal optics. The measured second-harmonic intensities also depend on other factors: reflection coefficients at the crystal/air interfaces, absorption and scattering of fundamental and second-harmonic light, etc. All of the foregoing is consistent with the powder technique affording qualitative information at best about the molecular properties of molecules in the crystals being investigated. In particular, observation of high power SHG is consistent with large β for a compound, while its absence does not necessarily preclude high molecular nonlinearities.

A major shortcoming of the technique is that materials which crystallize in centrosymmetric space groups theoretically cannot exhibit SHG, so the Kurtz method is only applicable to the ca. 20% of complexes that crystallize noncentrosymmetrically. However, despite the requirement for noncentrosymmetric crystal packing and the lack of a quantitative significance of the results, the Kurtz technique has been widely used because one can rapidly screen a large number of samples, and because one can conveniently study SHG without access to large single crystals.

3.2. Electric field-induced second-harmonic generation

Electric field-induced second-harmonic generation (EFISH) was used to measure molecular quadratic nonlinearities of metal acetylide complexes in early studies, but it has been largely superceded by the more widely applicable hyper-Rayleigh scattering technique. In the EFISH technique, the molecules in a solution of the complex are aligned using a high voltage dc pulse, which is synchronized with the laser beam pulse; this permits observation of $\chi^{(2)}$ in what was previously an isotropic medium. EFISH is formally a third-order nonlinear process described by the susceptibility $\chi^{(3)}(-2\omega; \omega, \omega, 0)$, so all materials will produce an EFISH

signal. There are two contributions to this susceptibility, one arising from the sum of the orientationally-averaged third-order hyperpolarizabilities $\gamma(-2\omega;\ \omega,\ \omega,\ 0)$ of the medium, and another due to the vectorial sum of the components of the second-order hyperpolarizabilities. Molecules with a permanent dipole μ partially align with the dc field. The net second-order effect is dependent on the $\boldsymbol{\mu}\cdot\boldsymbol{\beta}_{\text{vec}}$ product where $\boldsymbol{\mu}$ is the dipole moment of the molecule and $\boldsymbol{\beta}_{\text{vec}}$ is the vectorial component of the second-order hyperpolarizability (the hyperpolarizability β is a symmetric third-rank tensor that can be treated as being composed of a vector part and a septor part) [33]. In general, the directions of $\boldsymbol{\beta}_{\text{vec}}$ and of $\boldsymbol{\mu}$ are not coincident. The effective hyperpolarizability measured by the EFISH technique, β_{EFISH}, is given by $\boldsymbol{\mu}\cdot\boldsymbol{\beta}_{\text{vec}} = \mu\beta_{\text{EFISH}}$. For dipolar molecules containing strong electron donor and acceptor groups, β_{CT} (the hyperpolarizability along the charge-transfer axis) usually accounts for most of β_{EFISH}.

The solution of the sample is contained in a wedge shaped cell which is translated in a direction perpendicular to the incident laser beam. This creates Maker fringes whose periodicity is related to the wedge design and to the coherence length; the latter can therefore be determined. A measurement on a pure solvent is usually used to calibrate the system. The EFISH-derived third-order susceptibility $\Gamma = 3\chi^{(3)}(-2\omega;\ \omega, \omega, 0)$ is related to the molecular second hyperpolarizability γ' by local field factors and the molecule number density, and β can then be obtained from $\gamma' = \gamma + \mu\beta_{\text{EFISH}}/(5k_{\text{b}}T)$, where γ' is the effective second hyperpolarizability, γ is the intrinsic second hyperpolarizability (consisting of electronic and vibrational parts), k_{b} is Boltzmann's constant and T is the temperature in K. Comparison against a reference enables Γ values to be determined. EFISH measurements are usually performed as a function of concentration in a well-characterized solvent, a concentration dependence study being necessary to resolve ambiguities because the $\mu\beta_{\text{EFISH}}$ products for the solvent and the solute may be of the same or of opposite signs, and the SHG signal is proportional to the square of the EFISH susceptibility. Several other quantities may be required for the interpretation of the results: the dielectric constant, the permanent dipole moment, and the intrinsic second hyperpolarizability of the solute (found from a separate experiment or ignored).

EFISH has only been used to evaluate nonlinearities of neutral metal acetylide complexes, the presence of ionic species rendering it impossible to apply high electric fields to a solution. From the aforementioned description, it is clear that it is also not possible to utilize EFISH when the complex has no net dipole moment.

3.3. Hyper-Rayleigh scattering (HRS)

Hyper-Rayleigh scattering (HRS) has been (by far) the most widely utilized technique that has been employed to measure molecular quadratic nonlinearities of metal acetylide and vinylidene complexes. The HRS technique involves detecting the incoherently scattered second-harmonic light generated from an isotropic solution in order to determine the first hyperpolarizability. HRS arises from orientational fluctuations of unsymmetrical molecules in solution, resulting in local asymmetry in an isotropic liquid [34]. The scattered light can have a second-harmonic component that depends only on the first hyperpolarizability of the solute molecules, and varies quadratically with the incident intensity. The solute concentration is proportional to the square of the nonlinearity of all species in solution, and so varying the concentration of solutes allow β^2 to be extracted.

A schematic diagram of the HRS experiment is shown in Fig. 2. A seed injected, Q-switched laser pumps the HRS cell, the incident intensity and polarization being controlled by a half-wave plate polarizer combination and monitored by a photodiode or energy meter. The incident beam is focussed into the sample solution. A concave mirror, with its focus at the interaction focal volume, and a lens are used to collect the scattered light which is filtered to isolate the

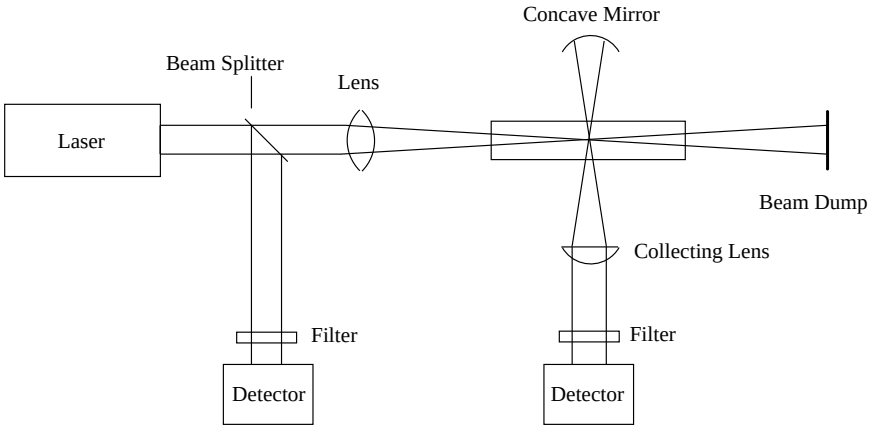

Fig. 2. Schematic diagram of the HRS experiment. Reproduced by permission of the American Institute of Physics from K. Clays and A. Persoons, Rev. Sci. Instrum. 63 (1992) 3286.

second-harmonic light, detected by a photomultiplier tube and averaged by a gated integrator.

HRS has a number of advantages compared to EFISH: it is simpler (a dc field is not required, and neither are measurements of μ or γ), it is sensitive to non-vector components of the β tensor, and one can measure octupolar molecules and ionic species, the last-mentioned being particularly important for organometallics with more than one accessible oxidation state. However, the need for sensitive detection and high intensity of the fundamental (due to the low intensity of the second-harmonic light) are disadvantages, the need for high intensity of the fundamental being particularly detrimental due to stimulated Raman or Brillouin scattering, self-focussing, or dielectric breakdown. Other disadvantages of HRS are that it is only possible to find the magnitude of β (this results from the quadratic dependence on the HRS signal) and that unreliable results are obtained when the complex fluoresces at the frequency-doubled wavelength.

3.4. Degenerate four-wave mixing

Degenerate four-wave mixing (DFWM) was used to measure molecular cubic nonlinearities of metal acetylide complexes in early studies, but it is now much less popular than the experimentally simpler Z-scan technique. In DFWM, two coherent "pump" beams interact within a material creating an interference pattern of light intensity. Because the change in refractive index of a third-order material depends on the intensity of the applied field, a refractive index grating results, which, in the simplest case, can be described by the dependence $\Delta n(r) = n_2 I(r)$. When a third beam is incident on this grating, a fourth beam is generated, the intensity of which is proportional to the product of all the input intensities and to the square of the absolute value of the complex third-order susceptibility, i.e. $I_4 \sim |\chi^{(3)}|^2 I_1 I_2 I_3$. In practice, one laser is used and the beam is split to provide the pump beams and the probe beam. DFWM has several advantages: one can measure all of the independent $\chi^{(3)}$ tensor components of an isotropic medium by using various combinations of polarizations for the four beams employed in the experiment, absolute and relative measurements of $\chi^{(3)}$ are possible [32], and the time dependence of the nonlinear response can be studied; the last-mentioned is significant because off-resonance electronic nonlinearities show a practically instantaneous response, and these can be separated from slower processes that also contribute to the nonlinear refractive index. One difficulty with DFWM is that, in order to distinguish between contributions from the real and imaginary part of the third-order susceptibility, one must perform a series of measurements on solutions of a compound with varying concentrations in a non-absorbing solvent. The concentration dependence of the DFWM signal is:

$$I_{\mathrm{DFWM}} \propto |\chi^{(3)}|^2 \propto [N_{\mathrm{solvent}}\gamma_{\mathrm{solvent}} + N_{\mathrm{solute}}\mathrm{Re}(\gamma_{\mathrm{solute}})]^2 + [N_{\mathrm{solute}}\mathrm{Im}(\gamma_{\mathrm{solute}})]^2$$

it being assumed that the solvent contributes only to the real part of the solution susceptibility, whereas the solute can contribute to both the real (refractive) and imaginary (absorptive) components.

Despite its experimental complexity, DFWM forms a complementary technique to the technically less difficult Z-scan, in that it can be used to verify that the origin of the observed nonlinearity is electronic in nature.

3.5. Z-scan

Z-scan is the technique that has been used to measure the cubic NLO merit of the vast majority of metal acetylide complexes studied thus far. It involves examining self-focussing or self-defocussing phenomena in a nonlinear material, from which one can derive the nonlinear refractive index intensity coefficient n_2 and thereby $\chi^{(3)}$ and γ [35]. Using a single Gaussian laser beam in a tight focus geometry (Fig. 3), the transmittance of a nonlinear medium through a fixed aperture in the far field is measured as the position of the material is varied. At the start (A) (and finish (E)) of the scan the sample is far removed from the focal plane. As a consequence, the intensity of the beam is low and lensing is not observed. As the material approaches the focal plane (B), lensing results in the beam focussing earlier, and the measured transmittance is thereby reduced. At the focal plane

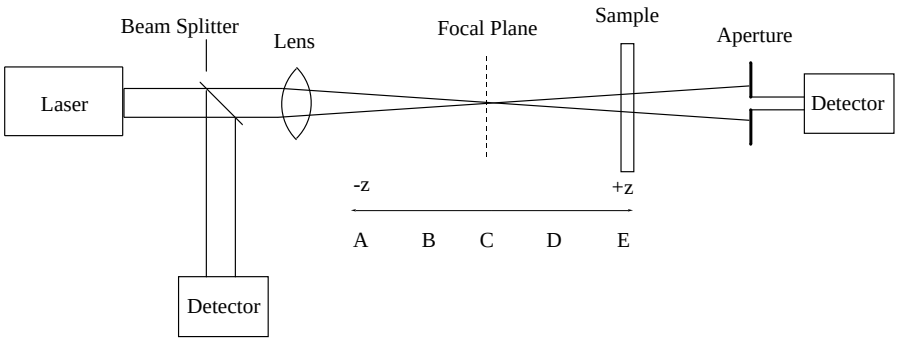

Fig. 3. Schematic diagram of the Z-scan experiment. Reprinted with permission from M. Skeik-Bahae, A.A. Said, T. Wei, D.J. Hagan and E.W. van Stryland, IEEE J. Quantam Electron. 26 (1990) 760. Copyright © 1990 IEEE.

(C), there is no change in transmittance, because a thin lens at the focus causes no change in the far-field. After the focal plane (D), focussing of the beam by the lensing of the material results in an increase in measured transmittance. The measured, normalized energy transmittance from a Z-scan experiment is numerically fitted to equations derived from theory, permitting the determination of n_2, $\chi^{(3)}$ and γ.

The shape of the Z-scan curve can be modified if nonlinear transmission (absorption bleaching) or nonlinear absorption occur, e.g. due to an imaginary component of $\chi^{(3)}$ of the material. The curves are then unsymmetrical because of increased transmission or absorption close to the focal plane. The nonlinear absorption coefficient β_2 or the related imaginary part of $\chi^{(3)}$ can be determined by analyzing the shape of such a modified Z-scan curve. An alternative experiment (usually referred to as an "open aperture Z-scan") can be used to determine the nonlinear absorption properties of a sample. In this experiment, the total intensity of the transmitted beam is measured without an aperture, as a function of the sample position with respect to the focal plane. Materials with potential optical limiting properties are often investigated by this means. For solutions, the nonlinearity changes on varying the concentration are determined, and hence measurements performed in an absolute manner, or, alternatively, results can be referenced to a standard.

There are several advantages of the Z-scan technique: the sign and magnitude of the nonlinear refractive index can be determined, both the real and imaginary parts of $\chi^{(3)}$ can be determined, and the single beam configuration results in simplicity (compared to DFWM). Z-scan also has disadvantages: a high quality Gaussian beam and good optical quality of samples are necessary, and the experiment does not afford information about the temporal nature of the nonlinear response.

3.6. Third-harmonic generation (THG)

Third-harmonic generation is employed to measure the electronic molecular second hyperpolarizability of centrosymmetric materials, because no process other than nonresonant electron cloud distortion responds sufficiently rapidly to produce a nonlinear polarization oscillating at the third harmonic [32]. All materials exhibit THG, including any glass used for a sample cell, or even air, so this experiment is technically difficult. One can avoid some problems by placing the sample in a vacuum sealed cell inside a vacuum chamber, but a simpler method involves using thick glass windows, permitting the contribution from air to be ignored; in this procedure, though, the third-order susceptibility of the glass and solvent must be known. THG has been used to study $\chi^{(3)}$ for several group 4 metal acetylides—it has not approached the popularity of the experimentally simpler Z-scan technique.

3.7. Optical Kerr gate

Optical Kerr gate (OKG) has been used less frequently than Z-scan for studies of metal acetylide complexes. In this experiment (Fig. 4), the sample is subjected to a linearly polarized pump beam which induces optical birefringence [32]. A probe beam of known linear polarization which is almost collinear with the pump beam then passes through the material, and the resultant light intensity through a crossed polarizer is measured. The Kerr gate transmittance is proportional to the square of the nonlinear phase shift between

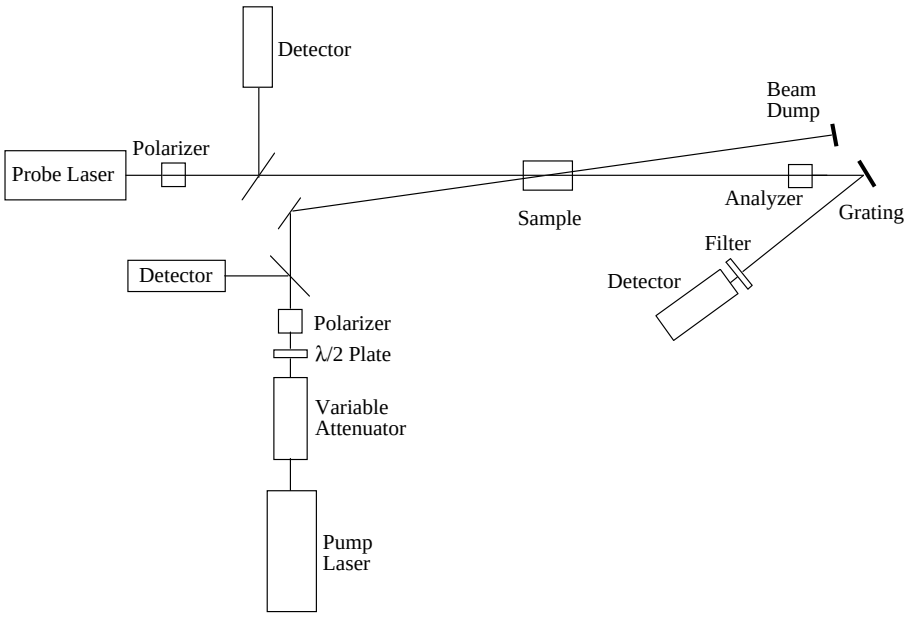

Fig. 4. Schematic diagram of an optical Kerr gate experiment. Reprinted from R.L. Sutherland, Handbook of Nonlinear Optics, Marcel Dekker, New York, 1996, p. 429, by courtesy of Marcel Dekker.

the slow and fast axes of the induced birefringence, with the phase shift itself being proportional to $(\chi^{(3)}_{xxyy} + \chi^{(3)}_{xyyx})I_{pump}$. Both the real and imaginary parts of $\chi^{(3)}$ contribute to the signal in the Kerr gate experiment, but a slightly modified experiment, heterodyne Kerr gate, can be used to resolve these two contributions. For electronic nonlinearity, the measured sum of the tensor components is equal to $\frac{2}{3}(\chi^{(3)}_{xxxx})$. An auxiliary experiment, polarization ellipse rotation, can be used to fully characterize the $\chi^{(3)}$ tensor. The Kerr gate experiments are slightly simpler than DFWM (although not as simple as Z-scan), both the real and imaginary parts of $\chi^{(3)}$ can be measured, and the temporal dependence of the nonlinear response can be studied, but the necessity to run two independent experiments to determine all the tensor components of $\chi^{(3)}$ has resulted in these techniques being significantly less popular because Z-scan and DFWM reveal more information from one experiment.

3.8. ZINDO (for calculating optical nonlinearities)

Computational techniques can afford insight into the structure–property relationships of molecules and materials, because the often time-consuming syntheses may be avoided by predicting responses computationally. Perhaps more importantly, otherwise inaccessible structural variations (such as bond length variation) may be probed. Unfortunately, though, modeling environmental interactions (intermolecular or solvent/molecule) is difficult [26,36,37], and so all calculated NLO responses of acetylide complexes are of individual molecules in the gas phase rather than of bulk materials. The only calculations of acetylide complexes thus far have employed ZINDO, which is a semi-empirical intermediate neglect of differential overlap/spectroscopy (INDO/S)-based routine. ZINDO utilizes a sum over excited particle hole states (SOS) method to calculate second-order nonlinear optical coefficients, and is parameterized to accommodate transition metal calculations. To achieve computational efficiency, some terms are replaced by empirical data or neglected. The SOS treatment is then used with the mono-excited state configuration interaction (MECI) approximation [38,39]. The values reported are β_{vec}, the value of β that lies along the dipolar axis (this is the value sampled by the EFISH technique), and β_{tot}, the total quadratic hyperpolarizability, which is defined as:

$$\beta_{tot} = \sqrt{(\beta_x^2 + \beta_y^2 + \beta_z^2)}$$

4. Second-order nonlinearities

4.1. Group 8 acetylide complexes

Complexes of the group 8 metals comprise the largest group of acetylide complexes to have been assessed for quadratic NLO merit, the results of these studies being collected in Table 1, and the structural formulas of some of the more efficient compounds being displayed in Fig. 5.

At this point it is apropos to mention that one must be very cautious in comparing results from different laboratories (perhaps obtained using different techniques and at different wavelengths); for example, [Fe(C≡CC$_6$H$_4$-4-NO$_2$)(dppe)(η^5-C$_5$H$_5$)] was measured in two laboratories in differing solvents and with differing references, and afforded data differing by up to a factor of two [50,95]. Dispersion is a serious concern: results are influenced by material resonances and the degree of this resonance enhancement is difficult to quantify. Dispersion of β for linear charge-transfer molecules can be described by a two state model, but such a model is probably not sufficient for metal acetylide complexes, and particularly octupolar examples. The two-level corrected β values (β_0) are available from:

$$\beta_0 = \beta\left(1 - \left(\frac{\lambda_{max}}{\lambda}\right)^2\right)\left(1 - \left(\frac{2\lambda_{max}}{\lambda}\right)^2\right)$$

where λ_{max} is the optical absorption maximum and λ is the fundamental wavelength of the laser. The β_0 values are listed in Table 1 and subsequent tables, but these data should be treated cautiously: three complexes in Table 1 have been examined by HRS at two wavelengths, the varying β_0 values testifying to the lack of applicability of the two-level model. The other major concern is that the various experimental techniques can sample different tensorial components or combinations thereof. Two complexes in Table 1 have been examined by both HRS and EFISH, the equivalent β values (within the experimental error margins) suggesting that there is one dominant tensor component ($\beta_{vec} = \beta_{EFISH} = \beta_{HRS} = \beta_{zzz}$).

Structure–NLO activity trends revealed from the data in Table 1 and subsequent tables in many cases mimic those found for organic molecules. It is helpful to note that the relationship between hyperpolarizabilities and linear optical absorption bands can be described by perturbation theory:

$$\beta \approx 3(\mu_{ee} - \mu_{gg})\left(\frac{\mu_{ge}^2}{E_{ge}^2}\right)$$

$$\gamma \propto \frac{-\mu_{ge}^4}{E_{ge}^3} + \frac{\mu_{ge}^2\mu_{ee'}^2}{E_{ge}^2 E_{ge'}} + \frac{\mu_{ge}^2(\mu_{ee} - \mu_{gg})^2}{E_{ge}^3}$$

where μ_{gg} is the ground state dipole moment, μ_{ee} is the excited state dipole moment, $\mu_{ee'}$ and μ_{ge} are transition dipole moments, and E_{ge} and $E_{ge'}$ are optical absorption energies. This provides a useful indication of factors influencing NLO merit to which the synthetic chemist can readily relate. For example, the former expression suggests that an intense (large μ_{ge}) charge-transfer (large $\mu_{ee} - \mu_{gg}$) transition at long wavelength (low E_{ge}) will correspond to a significant β coefficient. Not surprisingly, organic molecules containing conjugated π systems with unsymmetrical charge distribution have been shown to exhibit large second-order

Table 1
Molecular quadratic NLO measurements for group 8 acetylide complexes

Complex	λ_{max} (nm)	β[a] (10^{-30} esu)	β_0[a] (10^{-30} esu)	Technique	Solvent	Fund. (μm)	Ref.
[Fe(C≡CPh)(dppe)(η^5-C_5Me_5)]	348	52	24	HRS	CH_2Cl_2	1.064	[52]
1,3-C_6H_4[(C≡C)Fe(dppe)(η^5-C_5Me_5)]$_2$	349	210	98	HRS	CH_2Cl_2	1.064	[52]
1,3,5-C_6H_3[(C≡C)Fe(dppe)(η^5-C_5Me_5)]$_3$	351	175	87	HRS	CH_2Cl_2	1.064	[52]
1,4-C_6H_4[(C≡C)Fe(dppe)(η^5-C_5Me_5)]$_2$	413	180	60	HRS	CH_2Cl_2	1.064	[52]
(−)$_{436}$-*trans*-[Fe(C≡CC_6H_4-4-NO_2)Cl{(*R*,*R*)-diph}$_2$]	543	440	14	HRS	thf	1.064	[55]
[Fe(C≡CC_6H_4-4-NO_2)(CO)$_2$(η^5-C_5H_5)]	370	49	22	HRS	thf	1.064	[50]
[Fe(C≡CC_6H_4-4-NO_2)(dppe)(η^5-C_5H_5)]	498	665	64	HRS	thf	1.064	[50]
	504	1160	92	HRS	$CHCl_3$	1.064	[95]
[Fe(C≡CC_6H_4-4-C_6H_4-4-NO_2)(dppe)(η^5-C_5H_5)]	479	1150	173	HRS	$CHCl_3$	1.064	[95]
[Fe(C≡CC_6H_4-4-(*E*)-CH=CHC_6H_4-4-NO_2)(dppe)(η^5-C_5H_5)]	506	2315	171	HRS	$CHCl_3$	1.064	[95]
[Ru(C≡CPh)(PPh_3)$_2$(η^5-C_5H_5)]	310	89	45	HRS	thf	1.064	[46,56]
[Ru(C≡CC_6H_4-4-NO_2)(PPh_3)$_2$(η^5-C_5H_5)]	460	468	96	HRS	thf	1.064	[46,51]
[Ru(C≡CC_6H_4-4-NO_2)(PMe_3)$_2$(η^5-C_5H_5)]	477	248	39	HRS	thf	1.064	[46,51]
[Ru(C≡CC_6H_4-4-C≡CC_6H_4-4-NO_2)(PPh_3)$_2$(η^5-C_5H_5)]	448	560	134	HRS	thf	1.064	[46,56]
[Ru(C≡CC_6H_4-4-(*E*)-CH=CHC_6H_4-4-NO_2)(PPh_3)$_2$(η^5-C_5H_5)]	476	1455	232	HRS	thf	1.064	[46,51]
	476	1464	234	EFISH	thf	1.064	[46,51]
	484	2270	310	HRS	$CHCl_3$	1.064	[95]
	478	186	105	HRS	CH_2Cl_2	1.560	[43]
[Ru(C≡C-2-C_5H_4N)(PPh_3)$_2$(η^5-C_5H_5)]	331	18	10	HRS	thf	1.064	[40]
[Ru(C≡C-2-C_5H_3N-5-NO_2)(PPh_3)$_2$(η^5-C_5H_5)]	468	622	113	HRS	thf	1.064	[40]
[Ru(C≡CC_6H_4-4-C≡CC_6H_4-4-NO_2)(PPh_3)$_2$(η^5-C_5H_5)]	446	865	212	HRS	thf	1.064	[46,56]
[Ru(C≡CC_6H_4-4-N=CHC_6H_4-4-NO_2)(PPh_3)$_2$(η^5-C_5H_5)]	496	840	86	HRS	thf	1.064	[46,51]
	496	760	78	EFISH	thf	1.064	[46,51]
[Ru(C≡CC_6H_4-4-(*E*)-CH=CH-2-C_4H_2S-5-NO_2)(PPh_3)$_2$(η^5-C_5H_5)]	533	294	138	HRS	CH_2Cl_2	1.560	[43]
[Ru(C≡C-2-C_4H_2S-5-(*E*)-CH=CHC_6H_4-4-NO_2)(PPh_3)$_2$(η^5-C_5H_5)]	522	333	163	HRS	CH_2Cl_2	1.560	[43]
[Ru(C≡CC_6H_4-4-C≡C-2-C_4H_2S-5-NO_2)(PPh_3)$_2$(η^5-C_5H_5)]	505	210	109	HRS	CH_2Cl_2	1.560	[43]
[Ru{C≡C-(2-C_4H_2S-5-(*E*)-CH=CH)$_2$$C_6H_4$-4-$NO_2$}($PPh_3$)$_2$($\eta^5$-$C_5H_5$)]	536	419	195	HRS	CH_2Cl_2	1.560	[43]
[Ru(C≡CC_6H_4-4-N=CH-2-C_4H_2S-5-NO_2)(PPh_3)$_2$(η^5-C_5H_5)]	562	308	129	HRS	CH_2Cl_2	1.560	[43]
[Ru(C≡C-4-C_5H_4NMe)(PPh_3)$_2$(η^5-C_5H_5)][PF_6]	460	80	16	HRS	CH_2Cl_2	1.064	[57]
[Ru(C≡CC_6H_4-4-(*E*)-CH=CH-4-C_5H_4NMe)(PPh_3)$_2$(η^5-C_5H_5)][PF_6]	582	1600	154	HRS	CH_2Cl_2	1.064	[57]
[Ru(C≡CC_6H_4-4-C≡C-4-C_5H_4NMe)(PPh_3)$_2$(η^5-C_5H_5)][PF_6]	558	1400	102	HRS	CH_2Cl_2	1.064	[57]
[Ru(C≡CC_6H_4-4-NO_2)(PPh_3)$_2$(η^5-indenyl)]	476	746	119	HRS	CH_2Cl_2	1.064	[46,47]
[Ru(C≡CC_6H_4-4-NO_2)(dppe)(η^5-indenyl)]	459	516	107	HRS	CH_2Cl_2	1.064	[42]
[Ru(C≡CC_6H_4-4-NO_2)(dppm)(η^5-indenyl)]	456	540	117	HRS	CH_2Cl_2	1.064	[42]
[Ru(C≡C-(*E*)-CH=CHC_6H_4-4-NO_2)(PPh_3)$_2$(η^5-indenyl)]	507	1257	89	HRS	CH_2Cl_2	1.064	[42,47]
[Ru(C≡C-(*E*)-CH=CHC_6H_4-4-CN)(PPh_3)$_2$(η^5-indenyl)]	427	238	71	HRS	CH_2Cl_2	1.064	[42,47]
[Ru(C≡C-(*E*)-CH=CH-(*E*)-CH=CHC_6H_4-4-NO_2)(PPh_3)$_2$(η^5-indenyl)]	523	1320	34	HRS	CH_2Cl_2	1.064	[42,47]
[Ru(C≡C-(*E*)-CH=CH-4-C_5H_4N)(PPh_3)$_2$(η^5-indenyl)]	399	100	37	HRS	CH_2Cl_2	1.064	[46,47]
[Ru(C≡CC_6H_4-4-C≡CC_6H_4-4-NO_2)(PPh_3)$_2$(η^5-indenyl)]	463	1027	202	HRS	CH_2Cl_2	1.064	[42]
[Ru(C≡CC_6H_4-4-N=CHC_6H_4-4-NO_2)(PPh_3)$_2$(η^5-indenyl)]	509	1295	85	HRS	CH_2Cl_2	1.064	[42]
[Ru(C≡C-(*E*,*Z*)-CH=CH-2-C_4H_2O-5-NO_2)(PPh_3)$_2$(η^5-indenyl)]	550	908	43	HRS	CH_2Cl_2	1.064	[42]
[Ru(C≡C-(*E*)-CH=CH-2-C_4H_2S-5-NO_2)(PPh_3)$_2$(η^5-indenyl)]	598	487	88	HRS	CH_2Cl_2	1.064	[42]
[Ru{C≡CCH=C(C_6H_4-3-NO_2)$_2$}(PPh_3)$_2$(η^5-indenyl)]	345	48	25	HRS	CH_2Cl_2	1.064	[42]
[Ru{C≡C-(*E*)-CH=CH-4-C_5H_4N-1-Cr(CO)$_5$}(PPh_3)$_2$(η^5-indenyl)]	451	260	60	HRS	CH_2Cl_2	1.064	[42,47]
[Ru{C≡C-(*E*)-CH=CH-4-C_5H_4N-1-W(CO)$_5$}(PPh_3)$_2$(η^5-indenyl)]	462	535	71	HRS	CH_2Cl_2	1.064	[42,47]
[Ru{C≡C-(*E*)-CH=CHC_6H_4-4-C≡NCr(CO)$_5$}(PPh_3)$_2$(η^5-indenyl)]	442	465	119	HRS	CH_2Cl_2	1.064	[42,47]
[Ru{C≡C-(*E*)-CH=CHC_6H_4-4-C≡NW(CO)$_5$}(PPh_3)$_2$(η^5-indenyl)]	456	700	150	HRS	CH_2Cl_2	1.064	[42,47]
[Ru{C≡C-(*E*)-CH=CHC_6H_4-4-C≡NRu(NH_3)$_5$}(PPh_3)$_2$(η^5-indenyl)][CF_3SO_3]$_3$	442	315	80	HRS	Acetone	1.064	[42,47]
[Fe(η^5-C_5H_5){η^5-C_5H_4-(*E*)-CH=CHC≡CRu(PPh_3)$_2$(η^5-indenyl)}]	345	273	141	HRS	CH_2Cl_2	1.064	[42]
trans-[Ru(C≡CPh)Cl(dppm)$_2$]	308	20	12	HRS	thf	1.064	[41]
trans-[Ru(C≡CC_6H_4-4-NO_2)Cl(dppm)$_2$]	473	767	129	HRS	thf	1.064	[41]
trans-[Ru(C≡CC_6H_4-4-C_6H_4-4-NO_2)Cl(dppm)$_2$]	465	933	178	HRS	thf	1.064	[41]
trans-[Ru(C≡CC_6H_4-4-(*E*)-CH=CHC_6H_4-4-NO_2)Cl(dppm)$_2$]	490	1964	235	HRS	thf	1.064	[41]
trans-[Ru(C≡C-2-C_5H_4N)Cl(dppm)$_2$]	351	35	19	HRS	thf	1.064	[41]
trans-[Ru(C≡C-2-C_5H_3N-5-NO_2)Cl(dppm)$_2$]	490	468	56	HRS	thf	1.064	[41]
trans-[Ru(C≡CC_6H_4-4-C≡CPh)Cl(dppm)$_2$]	381	101	43	HRS	thf	1.064	[48]
trans-[Ru(C≡CC_6H_4-4-CHO)Cl(dppm)$_2$]	405	106	38	HRS	thf	1.064	[48]
trans-[Ru(C≡CC_6H_4-4-C≡CC_6H_4-4-NO_2)Cl(dppm)$_2$]	464	833	161	HRS	thf	1.064	[48]
trans-[Ru(C≡CC_6H_4-4-C≡CC_6H_4-4-C≡CC_6H_4-4-NO_2)Cl(dppm)$_2$]	439	1379	365	HRS	thf	1.064	[48]
trans-[Ru(C≡CPh)Cl(dppe)$_2$]	319	6	3	HRS	thf	1.064	[48]
trans-[Ru(C≡CC_6H_4-4-CHO)Cl(dppe)$_2$]	413	120	40	HRS	thf	1.064	[48]

Table 1 (*Continued*)

Complex	λ_{max} (nm)	β[a] (10^{-30} esu)	β_0[a] (10^{-30} esu)	Technique	Solvent	Fund. (μm)	Ref.
trans-[Ru(C≡CC_6H_4-4-NO_2)Cl(dppe)$_2$]	477	351	55	HRS	thf	1.064	[48]
trans-[Ru{C≡CC_6H_4-(*E*)-4-CH=CHC_6H_4-4-NO_2}Cl(dppe)$_2$]	489	2676	342	HRS	thf	1.064	[48]
[Ru{C≡CC_6H_4-(*E*)-4-N=NC_6H_4-4-NO_2}$(PPh_3)_2(\eta^5$-$C_5H_5)$]	565	1627	149	HRS	thf	1.064	[45]
trans-[Ru{C≡CC_6H_4-(*E*)-4-N=NC_6H_4-4-NO_2}Cl(dppm)$_2$]	583	1649	232	HRS	thf	1.064	[45]
[Ru{C≡CC_6H_4N=CCH=CBu^tC(O)C(Bu^t)=CH}$(PPh_3)_2(\eta^5$-$C_5H_5)$]	622	658	159	HRS	thf	1.064	[44]
[Ru{C≡CC_6H_4N=CCH=CBu^tC(O)C(Bu^t)=CH}Cl(dppm)$_2$]	645	417	124	HRS	thf	1.064	[44]
1,3,5-{*trans*-[RuCl(dppe)$_2$(C≡C-4-C_6H_4C≡C)]}$_3C_6H_3$	414	94	18	HRS	thf	1.064	[53]
1,3,5-{*trans*-[Ru(C≡CPh)(dppe)$_2$(C≡C-4-C_6H_4C≡C)]}$_3C_6H_3$	411	93	18	HRS	thf	1.064	[53]
trans-[Ru(C≡CPh)(C≡CC_6H_4-4-C≡CPh)(dppe)$_2$]	383	34	8	HRS	thf	1.064	[53]
trans-[Ru(C≡CPh)Cl(dppe)$_2$]	319	6	2	HRS	thf	1.064	[53]
[1-(HC≡C)-3,5-C_6H_3{*trans*-C≡CRuCl(dppm)$_2$}$_2$]	323	<42	<24	HRS	thf	1.064	[58]
trans-[Ru(C≡CC_6F_4-4-OMe)Cl(dppm)$_2$]	337	26	14	HRS	thf	1.064	[59]
trans-[Ru{C≡CC_6H_4-(*E*)-4-CH=CHPh}Cl(dppm)$_2$]	397	200 ± 40	44 ± 9	HRS	thf	1.064	[54]
	397	920[b]	5	HRS	thf	0.800	[54]
1,3,5-(*trans*-[RuCl(dppm)$_2${C≡CC_6H_4-(*E*)-4-CH=CH}$_3C_6H_3$	415	150 ± 92	28 ± 14	HRS	thf	1.064	[54]
	415	577 ± 19	16 ± 1	HRS	thf	0.800	[54]
$(-)_{578}$-*trans*-[Ru(C≡CPh)Cl{(*R*,*R*)-diph}$_2$]	292	too low	too low	HRS	thf	1.064	[55]
$(-)_{589}$-*trans*-[Ru(C≡CC_6H_4-4-NO_2)Cl{(*R*,*R*)-diph}$_2$]	467	530	97	HRS	thf	1.064	[55]
$(-)_{589}$-*trans*-[Ru(C≡CC_6H_4-(*E*)-4-CH=CHC_6H_4-4-NO_2)Cl{(*R*,*R*)-diph}$_2$]	481	2795	406	HRS	thf	1.064	[55]
[Ru(C≡CC_6H_4-4-NO_2)(CO)$_2(\eta^5$-$C_5H_5)$]	364	58	27	HRS	thf	1.064	[50]
[Ru(C≡CC_6H_4-4-NO_2)(dppe)$(\eta^5$-$C_5H_5)$]	447	664	161	HRS	thf	1.064	[50]
[Ru(C≡CC_6H_4-4-NO_2)$(PPh_3)_2(\eta^5$-$C_5H_5)$]	468	96	9	HRS	thf	1.064	[50]
[Ru(C≡CC_6H_4-4-CH{OC(O)Me}$_2$)$(PPh_3)_2(\eta^5$-$C_5H_5)$]	326	68	38	HRS	thf	1.064	[49]
[Ru(C≡CC_6H_4-4-CHO)$(PPh_3)_2(\eta^5$-$C_5H_5)$]	400	120	45	HRS	thf	1.064	[49]
trans-[Ru{C≡C-4-C_6H_4CHO(CHO(CH_2)$_3$O}Cl(dppm)$_2$]	320	61	35	HRS	thf	1.064	[49]
trans-[Ru(C≡CC_6H_4-3-CHO)Cl(dppm)$_2$]	321	58	34	HRS	thf	1.064	[49]
$(-)_{365}$-*trans*-[Os(C≡CC_6H_4-4-NO_2)Cl{(*R*,*R*)-diph}$_2$]	326	68	38	HRS	thf	1.064	[55]
[Os(C≡CC_6H_4-4-NO_2)(dppe)$(\eta^5$-$C_5H_5)$]	461	929	188	HRS	thf	1.064	[50]
[Os(C≡CC_6H_4-4-NO_2)$(PPh_3)_2(\eta^5$-$C_5H_5)$]	474	1051	174	HRS	thf	1.064	[50]

[a] β values have uncertainty of 10% unless otherwise noted.
[b] Upper bound only. No complete demodulation of the fluorescence contribution could be achieved.

NLO properties; thus, donor–acceptor substituted azo dyes, Schiff bases, and stilbenes, which are all molecules with easily polarizable π-electrons, all show large second-order nonlinearities. Nonlinearities can be enhanced by either increasing the conjugation length (improving delocalization) or increasing the strength of donor or acceptor groups (improving electron asymmetry). These NLO chromophore improvements result in a red-shift in the important linear optical absorption band, which reduces optical transparency, so octupolar molecules have been investigated in a bid to overcome this NLO efficiency/transparency trade off—the lack of a molecular dipole also improves the prospects of noncentrosymmetric crystal packing, required to manifest bulk susceptibility.

The data in Table 1 are consistent with an increase in β value upon increasing acetylide ligand chain length (proceeding from one-ring to biphenyl-, imino- and yne-linked two-ring acetylide ligand, with the azo- and ene-linked acetylide complexes the most efficient, and, indeed, more efficient than the complex with the three-ring yne-linked ligand); not surprisingly, an increase in β and β_0 value is seen on increasing n from 0 to 2 for *trans*-[Ru(C≡C(C_6H_4-4-C≡C)$_n C_6H_4$-4-NO_2)Cl(dppm)$_2$], although the β value for $n = 0$ and 1 are the same within the error margins. Ease of delocalization is enhanced upon replacing phenyl rings with heterocycles; however, nonlinearities do not consistently increase on replacing phenyl by pyridyl [40,41] and in fact, decrease on incorporation of an furanyl ring [42], while the location of the thienyl ring and phenyl ring in two-ring acetylide ligands was found to be unimportant in influencing NLO merit [43]. The use of iodoanilinoacetylide ligands such as in

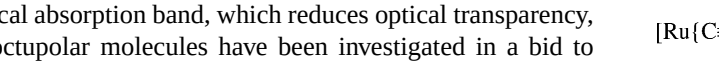

has been examined, because in the charge-transfer excited state the ring closer to the metal center becomes quinoidal, but the ring remote from the metal center becomes aromatic (Fig. 6), eliminating loss of aromatic stabilization energy and thereby enhancing nonlinearities. While the quadratic nonlinearity for this complex is large [44], it is not as large as similarly-sized two-ring azo- or ene-linked complexes [45].

Increasing the donor and/or acceptor strength generally results in an increase in nonlinearity. The 18 electron readily oxidizable ruthenium(II) centers in these complexes are very efficient donors—where direct comparison to related organic compounds is possible, it appears that the Ru(II) center is a stronger donor, resulting in large NLO coefficients. The efficient nitro group has been the

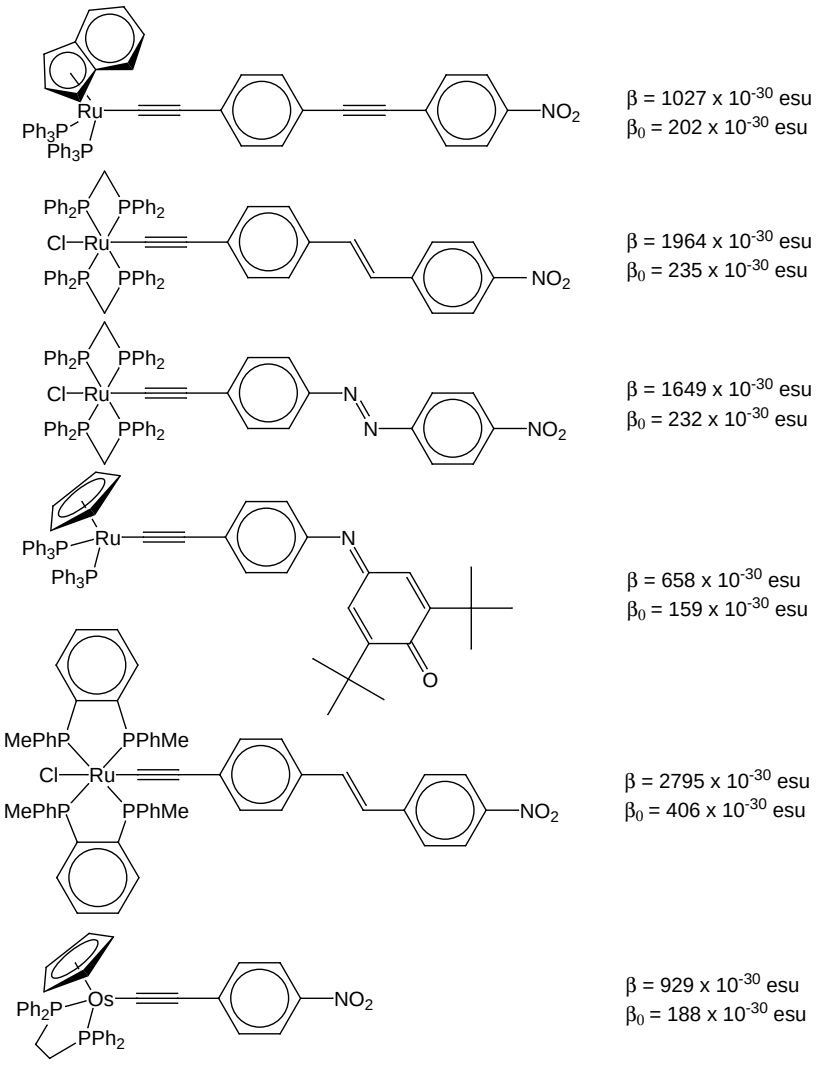

Fig. 5. Group 8 acetylide complexes with large β values.

most widely used acceptor across this series of complexes, replacement with other acceptor groups (CHO, CN) generally resulting in a decrease in nonlinearity, while alkylation of the 4-pyridylacetylide ligand to afford a 4-methylpyridinium acceptor afforded a complex with similar optical transparency to the 4-nitrophenylacetylide analogue, but greatly reduced nonlinearity. The 4-pyridyl group in [Ru{C≡C–(*E*)–CH=CH-4-C_5H_4N}$(PPh_3)_2(\eta^5$-indenyl)] has been metallated with $Cr(CO)_5$ and $W(CO)_5$ units, the products possessing considerably red-shifted linear absorption bands and significantly enhanced nonlinearities. Similarly, the nitrile group in [Ru{C≡C–(*E*)–CH=CH-4-C_6H_4CN}$(PPh_3)_2(\eta^5$-indenyl)] has been metallated with $Cr(CO)_5$, $W(CO)_5$ and $[Ru(NH_3)_5]^{3+}$ groups, with addition of the group 6 metals proving the more effective route to enhancing nonlinearities. In both cases, the tungsten-containing complexes are the more efficient [42,46,47]. It is also important to maintain conjugation

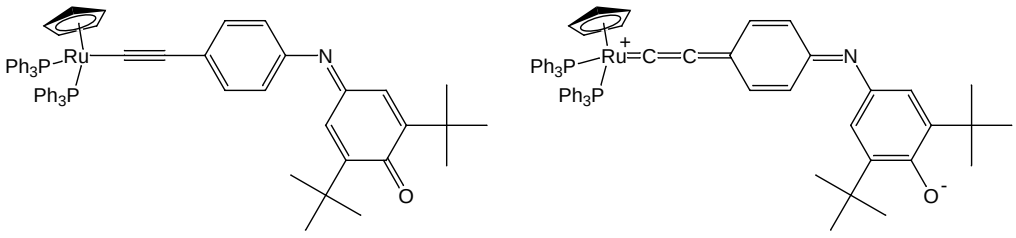

Fig. 6. Ground state (left) and charge-transfer excited state (right) representations of an indoanilinoacetylide complex.

pathway, replacement of C_6H_4-4-CHO with C_6H_4-3-CHO resulting in a decrease of the nonlinearity [48,49].

One advantage of organometallic complexes over organic compounds is the possibility of tuning NLO response by co-ligand modification. For the group 8 metal acetylide complexes, varying co-ligand should modify donor strength or delocalization possibilities. Replacing two CO ligands by dppe results in a significant increase in nonlinearity [50], while subtle variations (replacing dppe by dppm or two PPh_3 ligands) have no effect within the error margins. Interestingly, the nonlinearity for the triphenylphosphine complex is greater than that of the trimethylphosphine complex in the pair $[Ru(C{\equiv}CC_6H_4\text{-}4\text{-}NO_2)(L)_2(\eta^5\text{-}C_5H_5)]$, suggesting that the greater delocalization possibilities of the former are more important for NLO merit than the greater basicity of the latter [46,51]. Replacing the cyclopentadienyl by the indenyl ligand generally results in increased quadratic nonlinearity, while for metal variation the limited data thus far are unclear—some studies suggest increasing nonlinearity as β(iron complex) ≤ β(ruthenium complex) ≤ β(osmium complex) [42,46,47,50], whereas a further report suggests β(iron complex) > β(ruthenium complex) [95].

Recently, several octupolar acetylide complexes have been examined; their nonlinearities are modest [52–54], but none thus far incorporate acceptor groups at the core, introduction of which would be expected to enhance nonlinearity significantly. The "best" dipolar group 8 acetylide complexes represent the most efficient organometallic compounds with respect to quadratic NLO response, the β values being the same order of magnitude as the most efficient organic compounds.

4.2. Group 10 acetylide complexes

The molecular quadratic nonlinearities of a systematically varied series of (cyclopentadienyl)(triphenylphosphine)nickel acetylide complexes have been determined by hyper-Rayleigh scattering at 1.064 μm, the results being given in Table 2 and the structural formulas of some of the more efficient compounds being shown in Fig. 7. As with results for the ruthenium examples summarized above, dispersion-enhanced and two-level corrected nonlinearities increase upon introduction of acceptor substituent (nitro group), chain lengthening of acetylide ligand, and replacing *Z* by *E* stereochemistry at the acetylide ligand alkene linkage [40,60]. The nonlinearities for these 18-electron complexes are smaller than those for their 18-electron (cyclopentadienyl)bis(phosphine)ruthenium analogues, suggesting that the greater ease of oxidation of the latter is an important determinant of NLO merit in metal acetylide complexes [60].

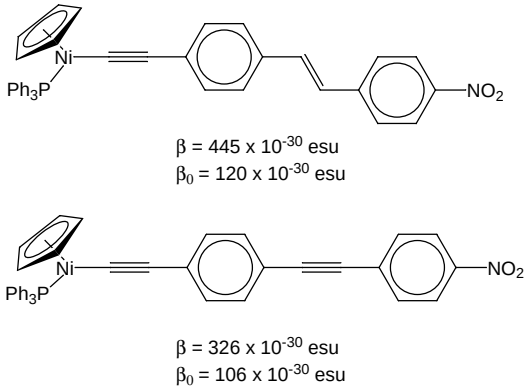

Fig. 7. Selected group 10 acetylides with high second-order optical nonlinearities.

4.3. Group 11 acetylide complexes

All group 11 acetylide complexes to have been examined thus far are (phosphine)gold complexes by HRS at 1.064 μm, the results of which are summarized in Table 3, while structural formulas of some of the more efficient complexes are displayed in Fig. 8. Unlike the other extensively investigated series (the ruthenium acetylide complexes), all of the gold complexes possess optical transitions in the UV and are optically transparent at the second-harmonic frequency. This is important as it permits a realistic evaluation of intrinsic off-resonance hyperpolarizabilities, and

Table 2
Molecular quadratic NLO measurements of group 10 acetylide complexes[a]

Complex	λ_{max} (nm)	β[b] (10^{-30} esu)	β_0[b] (10^{-30} esu)	Ref.
$[Ni(C{\equiv}CPh)(PPh_3)(\eta^5\text{-}C_5H_5)]$	307	24[c]	15	[60]
$[Ni(C{\equiv}CC_6H_4\text{-}4\text{-}NO_2)(PPh_3)(\eta^5\text{-}C_5H_5)]$	439	221	59	[60]
$[Ni(C{\equiv}CC_6H_4\text{-}4\text{-}C_6H_4\text{-}4\text{-}NO_2)(PPh_3)(\eta^5\text{-}C_5H_5)]$	413	193	65	[60]
$[Ni(C{\equiv}CC_6H_4\text{-}4\text{-}(E)\text{-}CH{=}CHC_6H_4\text{-}4\text{-}NO_2)(PPh_3)(\eta^5\text{-}C_5H_5)]$	437	445	120	[60]
$[Ni(C{\equiv}CC_6H_4\text{-}4\text{-}(Z)\text{-}CH{=}CHC_6H_4\text{-}4\text{-}NO_2)(PPh_3)(\eta^5\text{-}C_5H_5)]$	417	145	47	[60]
$[Ni(C{\equiv}CC_6H_4\text{-}4\text{-}C{\equiv}CC_6H_4\text{-}4\text{-}NO_2)(PPh_3)(\eta^5\text{-}C_5H_5)]$	417	326	106	[60]
$[Ni(C{\equiv}CC_6H_4\text{-}4\text{-}N{=}CHC_6H_4\text{-}4\text{-}NO_2)(PPh_3)(\eta^5\text{-}C_5H_5)]$	448	387	93	[60]
$[Ni(C{\equiv}C\text{-}2\text{-}C_5H_4N)(PPh_3)(\eta^5\text{-}C_5H_5)]$	415	25	8	[40]
$[Ni(C{\equiv}C\text{-}2\text{-}C_5H_3N\text{-}5\text{-}NO_2)(PPh_3)(\eta^5\text{-}C_5H_5)]$	456	186	41	[40]
$[1\text{-}(HC{\equiv}C)\text{-}3,5\text{-}C_6H_3\{C{\equiv}CNi(PPh_3)(\eta^5\text{-}C_5H_5)\}_2]$	316	94	55	[58]

[a] HRS, thf solvent, 1.064 μm.
[b] β values have uncertainty of 10% unless otherwise noted.
[c] Uncertainty of 20%.

Table 3
Molecular quadratic NLO measurements of group 11 acetylide complexes[a]

Complex	λ_{max} (nm)	β[b] (10^{-30} esu)	β_0[b] (10^{-30} esu)	Ref.
[Au(C≡CPh)(PPh_3)]	296	6	4	[46,61]
[Au(C≡CC_6H_4-4-NO_2)(PPh_3)]	338	22	12	[46,61]
[Au(C≡CC_6H_4-4-C_6H_4-4-NO_2)(PPh_3)]	350	39	20	[46,61]
[Au(C≡CC_6H_4-4-(*E*)-CH=CHC_6H_4-4-NO_2)(PPh_3)]	386	120	49	[46,61]
[Au(C≡CC_6H_4-4-(*Z*)-CH=CHC_6H_4-4-NO_2)(PPh_3)]	362	58	28	[46,61]
[Au(C≡CC_6H_4-4-C≡CC_6H_4-4-NO_2)(PPh_3)]	362	59	28	[46,61]
[Au(C≡CC_6H_4-4-N=CHC_6H_4-4-NO_2)(PPh_3)]	392	85	34	[46,61]
[Au(C≡CC_6H_4-4-(*E*)-N=NC_6H_4-4-NO_2)(PPh_3)]	398	180	68	[45]
[Au(C≡C-2-C_5H_4N)(PPh_3)]	300	7	4	[40]
[Au(C≡C-2-C_5H_3N-5-NO_2)(PPh_3)]	339	38	20	[40]
[Au(C≡C-2-C_5H_3N-5-NO_2)(PMe_3)]	340	12	6	[40]
[1,3,5-C_6H_3(C≡CAuPPh_3)$_3$]	298	6	4	[58]
[Au(C≡CC_6H_4-4-CHO)(PPh_3)]	322	14	8	[49]
[Au(C≡CC_6H_4-4-CHO)(PMe_3)]	322	[c]		[49]
[Au(C≡CC_6H_4-4-CHO$(CH_2)_3$O)(PPh_3)]	296	15	10	[49]
[Au(C≡CC_6H_4-4-CHO$(CH_2)_3$O)(PMe_3)]	292	48	31	[49]
[Au(C≡CC_6H_4-3-CHO)(PPh_3)]	318	[c]		[49]
[Au(C≡CC_6H_4-3-CHO)(PMe_3)]	322	[c]		[49]
[Au(C≡CC_6H_4-4-NO_2)(PCy_3)]	342	31	16	[62]
[Au(C≡CC_6H_4-4-NO_2)(PMe_3)]	339	50	27	[62]
[Au(C≡CC_6H_4-4-OMe)(PMe_3)]	339	44	25	[59]
[Au(C≡CC_6H_4-4-OMe)(PPh_3)]	296	20	14	[59]

[a] HRS, thf, 1.064 μm.
[b] β values have uncertainty of 10% unless otherwise noted.
[c] Too low to measure.

thereby reliable development of structure–NLO property relationships. The quadratic nonlinearities of these complexes show a similar dependence on the nature of the acetylide ligand as has been reported previously for organic chromophores. The efficiency sequence for acetylide ligand bridge variation C_6H_4 < $C_6H_4C_6H_4$ < $C_6H_4C{\equiv}CC_6H_4$ < *E*-$C_6H_4CH{=}CHC_6H_4$ was rationalized from π-bridge lengthening, torsion effects at the phenyl–phenyl linkage (of the biphenyl compound), and orbital energy mismatch of p orbitals of sp-hybridized acetylenic carbons with orbitals of sp^2 hybridized phenyl carbons (for the diphenylacetylene compound) [61]. Bridge stereochemistry affects quadratic nonlinearities as β(*Z* isomer) < β(*E* isomer), explained from a combination of greater dipole moment and more intense optical transition for the latter [61]. Quadratic nonlinearities are also observed to increase with increasing acceptor strength, viz. β(H) < β(CHO) < $\beta(NO_2)$ and for acceptor substitution site β(3-CHO) < β(4-CHO) [49]. The most efficient complex [Au(C≡CC_6H_4-4-(*E*)-N=NC_6H_4-4-NO_2)(PPh_3)] possesses the same acetylide ligand as one of the most efficient ruthenium acetylide complexes of similar size [45]; the efficiency of this ligand was predicted (before its synthesis) in earlier semi-empirical ZINDO studies [51].

4.4. Vinylidene complexes

Study of the quadratic NLO merit of vinylidene complexes is comparatively recent, significant impetus to this development being given from the interest in switching NLO properties coupled to the facile interconvertibility of acetylide and protonated vinylidene complex pairs via protonation/deprotonation sequences. Thus far, all reports are of ruthenium vinylidene complexes assessed by hyper-Rayleigh scattering at 1.064 μm, the results from which are collected in Table 4. The vinylidene complexes were not designed to have large quadratic NLO responses and, perhaps not surprisingly, nonlinearities for the monoruthenium vinylidene complexes are mostly low. Introduction of a nitro acceptor group results in increased β values. The octupolar complex [1,3,5-(*trans*-[RuCl(dppm)$_2${C=CHC_6H_4-(*E*)-4-CH=CH}])$_3C_6H_3$]$(PF_6)_3$ was examined by HRS with ns pulses at 1064 nm and fs pulses at 800 nm, the β values at the shorter wavelength being much greater, consistent with significant resonance enhancement resulting from close proximity of the optical absorption maximum to the second-harmonic wavelength of the latter (400 nm) [54].

The aryldiazovinylidene complexes are derivative of [Ru(C≡CPh)$(PPh_3)_2(\eta^5$-$C_5H_5)$] for which $\beta = 16 \times 10^{-30}$ esu ($\beta_0 = 10 \times 10^{-30}$ esu); an increase in β is observed upon introduction of functionalized aryldiazo group, but not upon incorporation of phenyldiazo unit. Complex [Ru(C=CPhN=NC_6H_4-4-NO_2)$(PPh_3)_2(\eta^5$-$C_5H_5)$]I was examined in three different solvents, nonlinearities varying as β(acetone) = $\beta(CH_2Cl_2)$ > β(thf). The molecular variation across these vinylidene complex salts affords trends in β consistent with the introduction of polarizing substituents

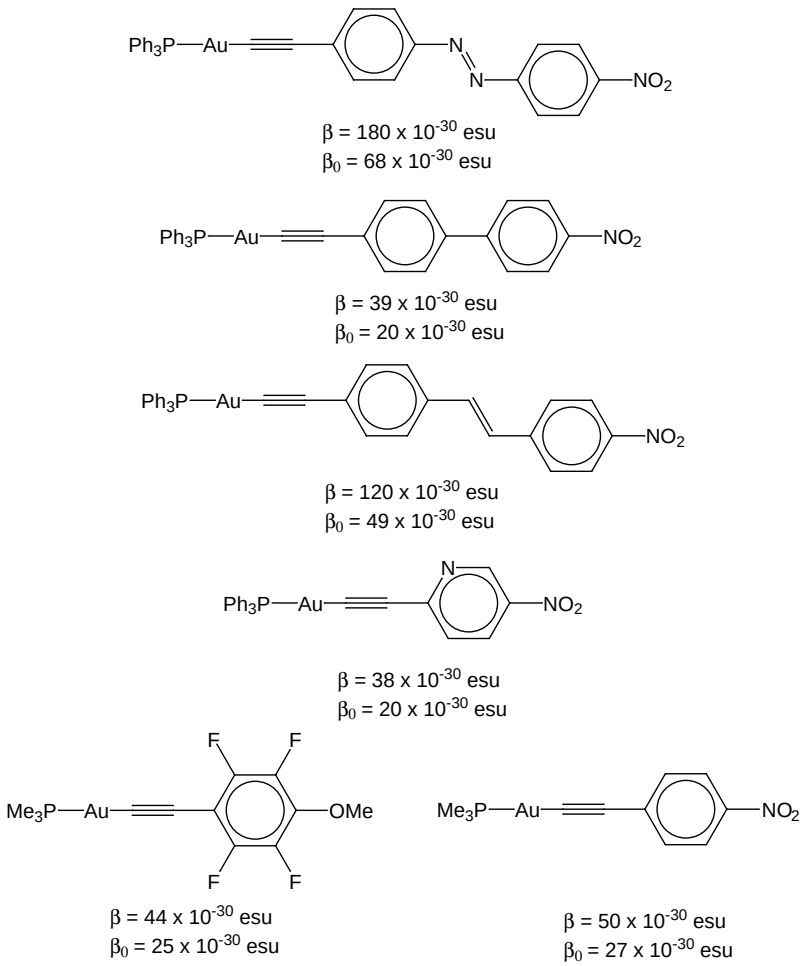

Fig. 8. Group 11 acetylide complexes with large β values.

(NO_2, OMe) and location of nitro substituent (4-NO_2 cf. 3,5-$(NO_2)_2$) making a significant contribution to the observed responses [63].

4.5. Kurtz powder measurements

The SHG efficiencies of more than forty acetylide or vinylidene complexes have been assessed using the Kurtz powder method, the results being listed in Table 5 and the structural formulas of the more efficient compounds being shown in Fig. 9.

In general, the bulk second-order data for vinylidene and acetylide complexes are disappointingly modest in comparison with literature-extant data for ferrocenyl complexes, for example, despite the fact that molecular quadratic nonlinearities for the more efficient acetylide complexes are significantly larger than those for the more efficient ferrocenyl complexes. The majority of the gold acetylide complexes to have been examined by the Kurtz technique decomposed. Strategies to engineer sizable $\chi^{(2)}$ values have been developed. For example, Marder et al. have shown that variation of counterions is a highly successful and very straightforward method to rapidly sample different lattice arrangements and thereby obtain materials with large nonlinearities [64]. This idea was utilized with the vinylidene complex cations, and proved its utility, but data for these salts of varying anion are uniformly low [65]. This strategy is not applicable to neutral complexes, although alternative procedures for organizing favorable lattice alignment have been developed, namely formation of guest–host inclusion complexes, and incorporation of chiral ligands. The former idea has not been pursued with vinylidene or acetylide complexes. The latter approach has been utilized using diph (1,2-bis(methylphenylphosphino)benzene) as the chiral ligand. For a variation in group 8 metal across the series *trans*-[$M(C{\equiv}CC_6H_4$-4-$NO_2)Cl\{(R,R)$-diph$\}_2$], the iron-containing complex has the largest Kurtz powder SHG efficiency, but its molecular nonlinearity is the lowest of the three complexes [55], emphasizing the fact that the usefulness of the Kurtz technique is to rapidly identify SHG activity; structure–NLO property correlations are not justified. The most SHG-efficient acetylide or vinylidene complex, [$Ni(C{\equiv}C$-2-C_5H_3N-5-$NO_2)(PPh_3)(\eta^5$-$C_5H_5)$], was shown to have a non-centrosymmetric crystal lattice, in a complementary X-ray diffraction study [40], but the acetylide chromophores were not aligned favorably.

Table 4
Molecular quadratic NLO measurements of vinylidene complexes[a]

Complex	λ_{max} (nm)	β[b] (10^{-30} esu)	β_0[b] (10^{-30} esu)	Solvent	Fund. (μm)	Ref.
trans-[Ru(C=CHC$_6$F$_4$-4-OMe)Cl(dppm)$_2$]PF$_6$	334	32	17	thf	1.064	[59]
trans-[Ru(C=CHC$_6$H$_4$-2-CHO)Cl(dppm)$_2$]PF$_6$	555	27	2	thf	1.064	[49]
trans-[Ru(C=CHC$_6$H$_4$-3-CHO)Cl(dppm)$_2$]PF$_6$	320	45	26	thf	1.064	[49]
trans-[Ru{C=CHC$_6$H$_4$-4-CHO(CH$_2$)$_3$O}Cl(dppm)$_2$]PF$_6$	317	64	38	thf	1.064	[49]
trans-[Ru(C=CHPh)Cl(dppm)$_2$]PF$_6$	320	24	16	thf	1.064	[48]
trans-[Ru(C=CHC$_6$H$_4$-4-C≡CPh)Cl(dppm)$_2$]PF$_6$	380	64	31	thf	1.064	[48]
trans-[Ru(C=CHC$_6$H$_4$-4-CHO)Cl(dppm)$_2$]PF$_6$	403	108	39	thf	1.064	[48]
trans-[Ru(C=CHC$_6$H$_4$-4-NO$_2$)Cl(dppm)$_2$]PF$_6$	470	721	127	thf	1.064	[48]
trans-[Ru(C=CHC$_6$H$_4$-4-C≡CC$_6$H$_4$-4-NO$_2$)Cl(dppm)$_2$]PF$_6$	326	424	122	thf	1.064	[48]
trans-[Ru{C=CHC$_6$H$_4$-4-(*E*)-CH=CHC$_6$H$_4$-4-NO$_2$)Cl(dppm)$_2$]PF$_6$	369	1899	314	thf	1.064	[48]
trans-[Ru(C=CHC$_6$H$_4$-4-CHO)Cl(dppe)$_2$]PF$_6$	412	181	61	thf	1.064	[48]
trans-[Ru(C=CHC$_6$H$_4$-4-NO$_2$)Cl(dppe)$_2$]PF$_6$	470	1130	180	thf	1.064	[48]
trans-[Ru{C=CHC$_6$H$_4$-4-(*E*)-CH=CHC$_6$H$_4$-4-NO$_2$)Cl(dppm)$_2$]PF$_6$	473	441	74	thf	1.064	[48]
[Ru(C=CHC$_6$H$_4$-4-NO$_2$)(PPh$_3$)$_2$(η^5-indenyl)]PF$_6$	379	116	50	CH_2Cl_2	1.064	[42,46,47]
[1,3,5-(*trans*-[RuCl(dppm)$_2${C=CHC$_6$H$_4$-(*E*)-4-CH=CH}])$_3$C$_6$H$_3$](PF$_6$)$_3$	396	165 ± 33	36 ± 7	thf	1.064	[54]
	396	101 ± 62[c]	22 ± 14	thf	1.064	[54]
	396	483 ± 100	4 ± 1	thf	0.800	[54]
	396	298 ± 62[c]	2 ± 1	thf	0.800	[54]
[Ru(C=CPhN=NPh)(PPh$_3$)$_2$(η^5-C$_5$H$_5$)]BF$_4$	363	14	6.6	Acetone	1.064	[63]
[Ru(C=CPhN=NC$_6$H$_4$-2-OMe)(PPh$_3$)$_2$(η^5-C$_5$H$_5$)]Cl	373	22	10	Acetone	1.064	[63]
[Ru(C=CPhN=NC$_6$H$_4$-3-OMe)(PPh$_3$)$_2$(η^5-C$_5$H$_5$)]BF$_4$	382	23	10	Acetone	1.064	[63]
[Ru(C=CPhN=NC$_6$H$_4$-4-OMe)(PPh$_3$)$_2$(η^5-C$_5$H$_5$)]Cl	370	26	12	Acetone	1.064	[63]
[Ru(C=CPhN=NC$_6$H$_4$-4-NO$_2$)(PPh$_3$)$_2$(η^5-C$_5$H$_5$)]BF$_4$	413	184	62	CH_2Cl_2	1.064	[63]
[Ru(C=CPhN=NC$_6$H$_4$-4-NO$_2$)(PPh$_3$)$_2$(η^5-C$_5$H$_5$)]Cl	413	137	46	CH_2Cl_2	1.064	[63]
[Ru(C=CPhN=NC$_6$H$_4$-4-NO$_2$)(PPh$_3$)$_2$(η^5-C$_5$H$_5$)]Br	413	136	45	CH_2Cl_2	1.064	[63]
[Ru(C=CPhN=NC$_6$H$_4$-4-NO$_2$)(PPh$_3$)$_2$(η^5-C$_5$H$_5$)]I	417	150	48	Acetone	1.064	[63]
	415	101	33	thf	1.064	[63]
	413	134	45	CH_2Cl_2	1.064	[63]
[Ru(C=CPhN=NC$_6$H$_4$-4-NO$_2$)(PPh$_3$)$_2$(η^5-C$_5$H$_5$)](4-MeC$_6$H$_4$SO$_3$)	413	164	55	CH_2Cl_2	1.064	[63]
[Ru(C=CPhN=NC$_6$H$_4$-4-NO$_2$)(PPh$_3$)$_2$(η^5-C$_5$H$_5$)]NO$_3$	413	181	61	CH_2Cl_2	1.064	[63]

[a] HRS.
[b] ±10% unless otherwise stated.
[c] $\sqrt{(\beta^2)}$.

Crystal engineering to convert large molecular nonlinearities into significant bulk nonlinearities remains a major challenge.

4.6. ZINDO-derived computational results

Table 6 contains data for computationally-derived second-order nonlinearities, obtained using ZINDO. Although ZINDO has been unsuccessful in reproducing absolute values of nonlinearities for acetylide complexes, a not-unexpected result when comparing resonance-enhanced solution-phase measurements in dipolar solvents with computationally-derived gas phase measurements far from resonance, it generally reproduces experimental trends. For example, for the acetylide complexes studied thus far, incorporation of a strong acceptor group and acetylide ligand chain lengthening both serve to increase nonlinearity, as expected [67,68]. The greatest utility of computational methods is in probing the effect of structural modifications that are not easy to accomplish experimentally. For example, Figs. 10 and 11 show the effect of Ru–C bond length variation and acetylide phenyl ring rotation upon ZINDO-derived β_{vec} values for [Ru(C≡CC$_6$H$_4$-4-NO$_2$)(PMe$_3$)$_2$(η^5-C$_5$H$_5$)], the calculations suggesting that one should minimize the Ru–C distance in order to maximize β_{vec}, and that the orientation of the phenylacetylide ligand with respect to the metal center is not an important concern for optimizing β_{vec}—the latter is a key result given difficulties in controlling ligand orientation in the crystal lattice [67].

5. Third-order nonlinearities

5.1. Group 4 acetylide complexes

The cubic nonlinearities of a series of group 4 metallocene acetylide complexes have been assessed by THG at 1.91 μm, results being displayed in Table 7. Although absolute values are low, some interesting trends in the data can be seen. Increasing nonlinearity is observed on replacing chloride by an acetylide ligand, butyl by phenyl substituent (acetylide variation), and in proceeding up the group upon metal replacement. The last-mentioned result was ascribed to two

Table 5
Kurtz powder measurements of acetylide or vinylidene complexes

Complex	SHG	Ref.
$(-)_{436}$-*trans*-[Fe(C≡CC_6H_4-4-NO_2)Cl{(*R*,*R*)-diph}$_2$]	∼2	[55]
$(-)_{589}$-*trans*-[Ru(C≡CC_6H_4-4-NO_2)Cl{(*R*,*R*)-diph}$_2$]	None detected	[55]
$(-)_{365}$-*trans*-[Os(C≡CC_6H_4-4-NO_2)Cl{(*R*,*R*)-diph}$_2$]	≪1	[55]
[Ru(C≡C-2-C_5H_3N)(PPh_3)$_2$(η5-C_5H_5)]	≪1	[40]
[Ru(C≡C-2-C_5H_3N-5-NO_2)(PPh_3)$_2$(η5-C_5H_5)]	≪1	[40]
[Ni(C≡C-2-C_5H_3N)(PPh_3)(η5-C_5H_5)]	≪1	[40]
[Ni(C≡C-2-C_5H_3N-5-NO_2)(PPh_3)(η5-C_5H_5)]	8	[40]
[Au(C≡C-2-C_5H_3N-5-NO_2)(PPh_3)]	≪1	[40]
[Au(C≡C-2-C_5H_3N-5-NO_2)(PMe_3)]	≪1	[40]
[Au(C≡CPh)(nmdpp)]	0	[66]
[Au(C≡CC_6H_4-4-NO_2)(nmdpp)]	2	[66]
[Au(C≡CC_6H_4-4-C_6H_4-4-NO_2)(nmdpp)]	<1, fluoresced, decomposed	[66]
[Au(C≡CC_6H_4-(*E*)-4-CH=CHC_6H_4-4-NO_2)(nmdpp)]	<1, fluoresced, decomposed	[66]
[Au(C≡CC_6H_4-(*Z*)-4-CH=CHC_6H_4-4-NO_2)(nmdpp)]	<1, fluoresced, decomposed	[66]
[Au(C≡CC_6H_4-4-C≡CC_6H_4-4-NO_2)(nmdpp)]	<1, fluoresced, decomposed	[66]
[Au(C≡CC_6H_4-4-N=CHC_6H_4-4-NO_2)(nmdpp)]	<1, fluoresced, decomposed	[66]
[Au(C≡CPh)(PPh_3)]	0	[66]
[Au(C≡CC_6H_4-4-NO_2)(PPh_3)]	0	[66]
[Au(C≡CC_6H_4-4-C_6H_4-4-NO_2)(PPh_3)]	Fluoresced, decomposed	[66]
[Au(C≡CC_6H_4-(*E*)-4-CH=CHC_6H_4-4-NO_2)(PPh_3)]	Fluoresced, decomposed	[66]
[Au(C≡CC_6H_4-(*Z*)-4-CH=CHC_6H_4-4-NO_2)(PPh_3)]	Fluoresced, decomposed	[66]
[Au(C≡CC_6H_4-4-C≡CC_6H_4-4-NO_2)(PPh_3)]	Fluoresced, decomposed	[66]
[Au(C≡CC_6H_4-4-N=CHC_6H_4-4-NO_2)(PPh_3)]	Fluoresced, decomposed	[66]
[Ru(C=CPhN=NPh)(PPh_3)$_2$(η^5-C_5H_5)]BF_4	0.48	[65]
[Ru(C=CPhN=NPh)(PPh_3)$_2$(η^5-C_5H_5)](4-$MeC_6H_4SO_3$)	0.50	[65]
[Ru(C=CPhN=NPh)(PPh_3)$_2$(η^5-C_5H_5)]NO_3	0.57	[65]
[Ru(C=CPhN=NPh)(PPh_3)$_2$(η^5-C_5H_5)]Cl	0.50	[65]
[Ru(C=CPhN=NPh)(PPh_3)$_2$(η^5-C_5H_5)]I	0.53	[65]
[Ru(C=CPhN=NC_6H_4-4-OMe)(PPh_3)$_2$(η^5-C_5H_5)]BF_4	1.05	[65]
[Ru(C=CPhN=NC_6H_4-4-OMe)(PPh_3)$_2$(η^5-C_5H_5)](4-$MeC_6H_4SO_3$)	<0.05	[65]
[Ru(C=CPhN=NC_6H_4-4-OMe)(PPh_3)$_2$(η^5-C_5H_5)]NO_3	<0.05	[65]
[Ru(C=CPhN=NC_6H_4-4-OMe)(PPh_3)$_2$(η^5-C_5H_5)]Cl	<0.05	[65]
[Ru(C=CPhN=NC_6H_4-4-OMe)(PPh_3)$_2$(η^5-C_5H_5)]I	<0.05	[65]
[Ru(C=CPhN=NC_6H_4-2-OMe)(PPh_3)$_2$(η^5-C_5H_5)]BF_4	0.63	[65]
[Ru(C=CPhN=NC_6H_4-2-OMe)(PPh_3)$_2$(η^5-C_5H_5)](4-$MeC_6H_4SO_3$)	<0.05	[65]
[Ru(C=CPhN=NC_6H_4-2-OMe)(PPh_3)$_2$(η^5-C_5H_5)]NO_3	<0.05	[65]
[Ru(C=CPhN=NC_6H_4-2-OMe)(PPh_3)$_2$(η^5-C_5H_5)]Cl	<0.05	[65]
[Ru(C=CPhN=NC_6H_4-2-OMe)(PPh_3)$_2$(η^5-C_5H_5)]I	<0.05	[65]
[Ru(C=CPhN=NC_6H_4-4-NO_2)(PPh_3)$_2$(η^5-C_5H_5)]BF_4	<0.05	[65]
[Ru(C=CPhN=NC_6H_4-4-NO_2)(PPh_3)$_2$(η^5-C_5H_5)](4-$MeC_6H_4SO_3$)	<0.05	[65]
[Ru(C=CPhN=NC_6H_4-4-NO_2)(PPh_3)$_2$(η^5-C_5H_5)]NO_3	<0.05	[65]
[Ru(C=CPhN=NC_6H_4-4-NO_2)(PPh_3)$_2$(η^5-C_5H_5)]Cl	<0.05	[65]
[Ru(C=CPhN=NC_6H_4-4-NO_2)(PPh_3)$_2$(η^5-C_5H_5)]I	<0.05	[65]
[Ru(C=CPhN=NC_6H_3-3,5-$(NO_2)_2$)(PPh_3)$_2$(η^5-C_5H_5)]BF_4	<0.05	[65]
[Ru(C=CPhN=NC_6H_3-3,5-$(NO_2)_2$)(PPh_3)$_2$(η^5-C_5H_5)](4-$MeC_6H_4SO_3$)	<0.05	[65]
[Ru(C=CPhN=NC_6H_3-3,5-$(NO_2)_2$)(PPh_3)$_2$(η^5-C_5H_5)]NO_3	<0.05	[65]
[Ru(C=CPhN=NC_6H_3-3,5-$(NO_2)_2$)(PPh_3)$_2$(η^5-C_5H_5)]Cl	<0.05	[65]
[Ru(C=CPhN=NC_6H_3-3,5-$(NO_2)_2$)(PPh_3)$_2$(η^5-C_5H_5)]I	<0.05	[65]

factors: the involvement of ligand-to-metal charge-transfer transition for these complexes, and increasing electron accepting ability of the metal [70].

5.2. Group 8 acetylide complexes

Group 8 acetylide complexes have been intensively studied for their third-order NLO properties; the results of studies, almost all on ruthenium acetylide compounds and all but one by Z-scan at 0.80 μm, are collected in Table 8, while structural formulas of some of the more efficient examples are displayed in Fig. 12. One complex, [Ru(C≡CC_6H_4-4-NO_2)(PPh_3)$_2$(η^5-C_5H_5)], has been examined by both Z-scan and DFWM; the latter study revealed an equivalent γ value (within the error margins) to the Z-scan-derived response, and confirmed an electronic origin for cubic NLO response in this molecule [73].

While less is known of molecular structure–NLO activity relationships for third-order properties than for second-order properties, it has been established with organic compounds

Table 6
Computationally-derived optical nonlinearities by ZINDO for acetylide complexes[a]

Complex	β_{vec} (10^{-30} esu)	Ref.
$[Ru(C{\equiv}CPh)(PPh_3)_2(\eta^5\text{-}C_5H_5)]$	2	[67]
$[Ru(C{\equiv}CPh)(PMe_3)_2(\eta^5\text{-}C_5H_5)]$	5	[67]
$[Ru(C{\equiv}CC_6H_4\text{-}4\text{-}NO_2)(PPh_3)_2(\eta^5\text{-}C_5H_5)]$	29	[67]
$[Ru(C{\equiv}CC_6H_4\text{-}4\text{-}NO_2)(PMe_3)_2(\eta^5\text{-}C_5H_5)]$	31	[67]
trans-$[Ru(C{\equiv}CPh)Cl(dppm)_2]$	−13	[68]
trans-$[Ru(C{\equiv}CC_6H_4\text{-}4\text{-}NO_2)Cl(dppm)_2]$	34	[68]
trans-$[Ru(C{\equiv}CC_6H_4\text{-}4\text{-}C_6H_4\text{-}4\text{-}NO_2)Cl(dppm)_2]$	45	[68]
trans-$[Ru(C{\equiv}CC_6H_4\text{-}(E)\text{-}4\text{-}CH{=}CHC_6H_4\text{-}4\text{-}NO_2)Cl(dppm)_2]$	60	[68]
trans-$[Ru(C{\equiv}CC_6H_4\text{-}4\text{-}NO_2)_2(dppm)_2]$	0	[69]
trans-$[Ru(C{\equiv}CPh)(C{\equiv}CC_6H_4\text{-}4\text{-}NO_2)(dppm)_2]$	32	[69]

[a] 1.91 μm.

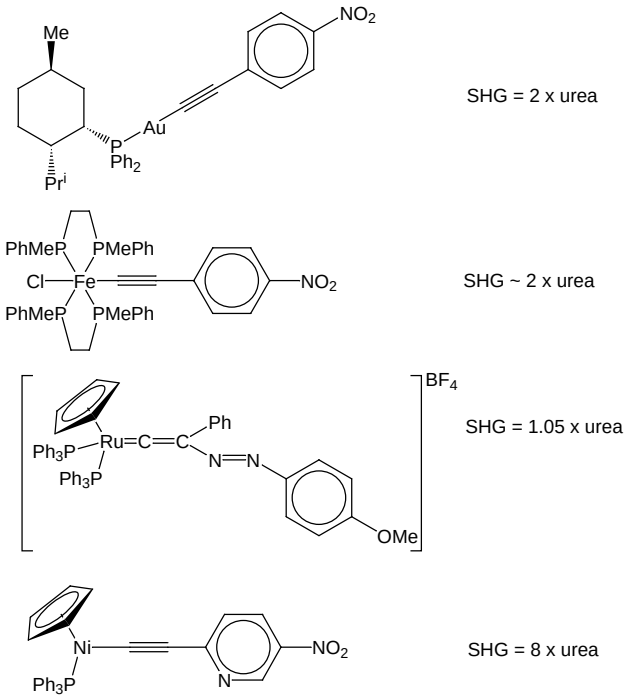

Fig. 9. Acetylide or vinylidene complexes with the largest $\chi^{(2)}$ values measured by the Kurtz powder technique.

that increase in π-delocalization possibilities (e.g. progressing from small molecules to π-conjugated polymers), the introduction of strong donor and acceptor functional groups, controlling chain orientation, packing density, and

Table 7
Molecular cubic NLO measurements of group 4 acetylide complexes[a]

Complex	λ (nm)	γ (10^{-36} esu)	Ref.
$[Ti(C{\equiv}CBu^n)_2(\eta^5\text{-}C_5H_4Me)_2]$	[b]	15 ± 2	[71]
$[Ti(C{\equiv}CBu^n)_2(\eta^5\text{-}C_5H_5)_2]$	390	12 ± 2	[72]
$[Ti(C{\equiv}CPh)_2(\eta^5\text{-}C_5H_5)_2]$	416	92 ± 14	[70,71]
$[Zr(C{\equiv}CPh)_2(\eta^5\text{-}C_5H_5)_2]$	390	58 ± 9	[70,71]
$[Hf(C{\equiv}CPh)_2(\eta^5\text{-}C_5H_5)_2]$	390	51 ± 8	[70,71]
$[Ti(C{\equiv}CPh)Cl(\eta^5\text{-}C_5H_5)_2]$	510	31 ± 5	[70,71]

[a] THG, 1.91 μm.
[b] Not reported.

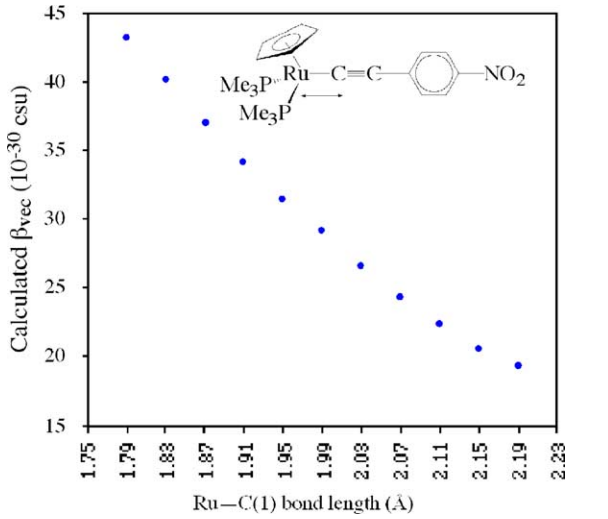

Fig. 10. The effect of varying Ru–C bond length on ZINDO-derived quadratic nonlinearity for $[Ru(C{\equiv}CC_6H_4\text{-}4\text{-}NO_2)(PMe_3)_2(\eta^5\text{-}C_5H_5)]$. Reprinted with permission from I.R. Whittall, M.G. Humphrey, D.C.R. Hockless, B.W. Skelton and A.H. White, Organometallics 14 (1995) 3978. Copyright © 1995 American Chemical Society.

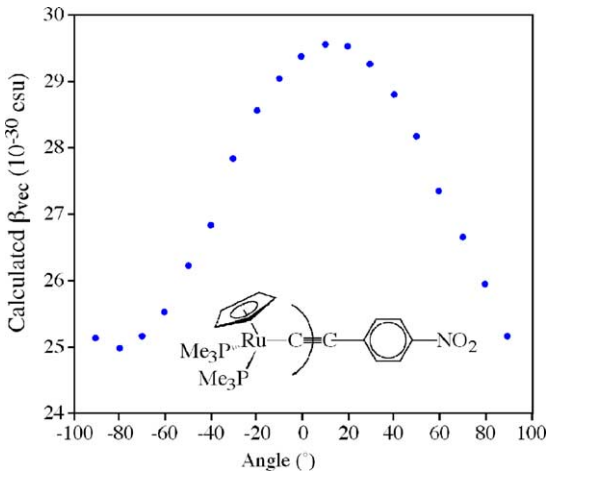

Fig. 11. The effect of nitrophenylacetylide ligand rotation on ZINDO-derived quadratic nonlinearity for $[Ru(C{\equiv}CC_6H_4\text{-}4\text{-}NO_2)(PMe_3)_2(\eta^5\text{-}C_5H_5)]$. Reprinted with permission from I.R. Whittall, M.G. Humphrey, D.C.R. Hockless, B.W. Skelton and A.H. White, Organometallics 14 (1995) 3978. Copyright © 1995 American Chemical Society.

Table 8
Molecular cubic NLO measurements of group 8 acetylide complexes

Complex	λ_{max} (nm)	γ_{real} (10^{-36} esu)	γ_{imag} (10^{-36} esu)	γ (10^{-36} esu)	Technique	Solvent	Fund. (μm)	Ref.
[Fe(C≡CC$_6$H$_4$-4-NO$_2$)(dppe)(η^5-C$_5$H$_5$)]	497	−410 ± 200	580 ± 200	710 ± 280	Z-scan	thf	0.80	[95]
[Fe(C≡CC$_6$H$_4$-4-(*E*)-CH=CHC$_6$H$_4$-4-NO$_2$)(dppe)(η^5-C$_5$H$_5$)]	499	−2200 ± 600	1200 ± 300	2500 ± 670	Z-scan	thf	0.80	[95]
[Ru(C≡CPh)(PPh$_3$)$_2$(η^5-C$_5$H$_5$)]	311	≤150		≤150	Z-scan	thf	0.80	[73]
[Ru(C≡CC$_6$H$_4$-4-Br)(PPh$_3$)$_2$(η^5-C$_5$H$_5$)]	325	≤150		≤150	Z-scan	thf	0.80	[73]
[Ru(C≡CC$_6$H$_4$-4-NO$_2$)(PPh$_3$)$_2$(η^5-C$_5$H$_5$)]	461	−210 ± 50	≤10	−210 ± 50	Z-scan	thf	0.80	[73]
	461	−260 ± 60		−260 ± 60	DFWM	thf	0.80	[73]
[Ru(C≡CC$_6$H$_4$-4-NO$_2$)(PMe$_3$)$_2$(η^5-C$_5$H$_5$)]	480	−230 ± 70	74 ± 30	240 ± 76	Z-scan	thf	0.80	[73]
[Ru(C≡CC$_6$H$_4$-4-C$_6$H$_4$-4-NO$_2$)(PPh$_3$)$_2$(η^5-C$_5$H$_5$)]	448	−380 ± 200	320 ± 160	500 ± 260	Z-scan	thf	0.80	[73]
[Ru(C≡CC$_6$H$_4$-4-(*E*)-CH=CHC$_6$H$_4$-4-NO$_2$)(PPh$_3$)$_2$(η^5-C$_5$H$_5$)]	476	−450 ± 100	210 ± 100	500 ± 140	Z-scan	thf	0.80	[73]
[Ru(C≡CC$_6$H$_4$-4-C≡CC$_6$H$_4$-4-NO$_2$)(PPh$_3$)$_2$(η^5-C$_5$H$_5$)]	447	−450 ± 100	≤20	−450 ± 100	Z-scan	thf	0.80	[73]
[Ru(C≡CC$_6$H$_4$-4-N=CHC$_6$H$_4$-4-NO$_2$)(PPh$_3$)$_2$(η^5-C$_5$H$_5$)]	496	−850 ± 300	360 ± 200	920 ± 360	Z-scan	thf	0.80	[56]
trans-[Ru(C≡CC$_6$H$_4$-4-NO$_2$)Cl(dppm)$_2$]	466	170 ± 34	230 ± 46	290 ± 57	Z-scan	CH_2Cl_2	0.80	[75]
trans-[Ru(C≡CC$_6$H$_4$-4-C$_6$H$_4$-4-NO$_2$)Cl(dppm)$_2$]	448	140 ± 28	64 ± 13	150 ± 31	Z-scan	CH_2Cl_2	0.80	[75]
trans-[Ru(C≡CC$_6$H$_4$-4-(*E*)-CH=CHC$_6$H$_4$-4-NO$_2$)Cl(dppm)$_2$]	471	200 ± 40	1100 ± 220	1100 ± 220	Z-scan	CH_2Cl_2	0.80	[75]
trans-[Ru(C≡CC$_6$H$_4$-4-NO$_2$)$_2$(dppm)$_2$]	474	300 ± 60	490 ± 98	570 ± 110	Z-scan	CH_2Cl_2	0.80	[75]
trans-[Ru(C≡CC$_6$H$_4$-4-C$_6$H$_4$-4-NO$_2$)$_2$(dppm)$_2$]	453	≤800	2500 ± 500	2500 ± 500	Z-scan	CH_2Cl_2	0.80	[75]
trans-[Ru(C≡CC$_6$H$_4$-4-(*E*)-CH=CHC$_6$H$_4$-4-NO$_2$)$_2$(dppm)$_2$]	367	≤1100	3400 ± 680	3400 ± 680	Z-scan	CH_2Cl_2	0.80	[75]
1,3,5-{*trans*-[RuCl(dppe)$_2$(C≡CC$_6$H$_4$-4-C≡C)}$_3$C$_6$H$_3$	414	−330 ± 100	2200 ± 500	2200 ± 600	Z-scan	thf	0.80	[53]
1,3,5-{*trans*-[Ru(C≡CPh)(dppe)$_2$(C≡CC$_6$H$_4$-4-C≡C)}$_3$C$_6$H$_3$	411	−600 ± 200	2900 ± 500	3000 ± 600	Z-scan	thf	0.80	[53]
1-(Me$_3$SiC≡C)-C$_6$H$_3$-3,5-{C≡CC$_6$H$_4$-4-C≡C-*trans*-[RuCl(dppe)$_2$]}$_2$	411	−510 ± 500	4700 ± 1500	4700 ± 2000	Z-scan	thf	0.80	[74]
1-(Me$_3$SiC≡C)-C$_6$H$_3$-3,5-{C≡CC$_6$H$_4$-4-C≡C-*trans*-[Ru(C≡CPh)(dppe)$_2$]}$_2$	407	−700 ± 100	2270 ± 300	2400 ± 300	Z-scan	thf	0.80	[74]
1-(HC≡C)-C$_6$H$_3$-3,5-{C≡CC$_6$H$_4$-4-C≡C-*trans*-[Ru(C≡CPh)(dppe)$_2$]}$_2$	408	−830 ± 100	2200 ± 300	2400 ± 300	Z-scan	thf	0.80	[74]
1,3,5-C$_6$H$_3$-(C≡CC$_6$H$_4$-4-C≡C-*trans*-[Ru(dppe)$_2$]C≡C-3,5-C$_6$H$_3$-{C≡CC$_6$-H$_4$-4-C≡C-*trans*-[Ru(C≡CPh)(dppe)$_2$]$_2$})$_3$	402	−5050 ± 500	20100 ± 2000	20700 ± 2000	Z-scan	thf	0.80	[74]
trans-[Ru(C≡CPh)(C≡CC$_6$H$_4$-4-C≡CPh)(dppe)$_2$]	383	−670 ± 300	1300 ± 300	1500 ± 500	Z-scan	CH_2Cl_2	0.80	[53]
trans-[Ru(C≡CPh)Cl(dppe)$_2$]	319	−170 ± 40	71 ± 20	200 ± 50	Z-scan	CH_2Cl_2	0.80	[53]
trans-[Ru{C≡CC$_6$H$_4$-(*E*)-4-CH=CHPh}Cl(dppm)$_2$]	397	−600 ± 400	700 ± 400	920 ± 600	Z-scan	thf	0.80	[54,76]
trans-[Ru{C≡CC$_6$H$_4$-(*E*)-4-CH=CHPh}Cl(dppe)$_2$]	404	300 ± 400	300 ± 100	420 ± 350	Z-scan	thf	0.80	[54,76]
1,3,5-(*trans*-[RuCl(dppm)$_2${4-C≡CC$_6$H$_4$-(*E*)-4-CH=CH}])$_3$C$_6$H$_3$	415	−640 ± 500	2000 ± 500	2100 ± 600	Z-scan	thf	0.80	[54,76]
1,3,5-(*trans*-[RuCl(dppe)$_2${C≡CC$_6$H$_4$-(*E*)-4-CH=CH}])$_3$C$_6$H$_3$	426	−4600 ± 2000	4200 ± 800	6200 ± 2000	Z-scan	thf	0.80	[54,76]
1,3,5-(*trans*-[Ru(C≡CPh)(dppe)$_2${C≡CC$_6$H$_4$-(*E*)-4-CH=CH}])$_3$C$_6$H$_3$	421	−11200 ± 3000	8600 ± 2000	14000 ± 4000	Z-scan	thf	0.80	[54,76]
[Fe{η^5-C$_5$H$_4$-(*E*)-CH=CHC$_6$H$_4$-4-C≡CRuCl(dppm)$_2$}$_2$]	396	−3000 ± 1200	2300 ± 800	3800 ± 1400	Z-scan	thf	0.80	[77]
[Fe{η^5-C$_5$H$_4$-(*E*)-CH=CHC$_6$H$_4$-4-C≡CRuCl(dppe)$_2$}$_2$]	388	−7100 ± 3000	10600 ± 2000	13000 ± 3000	Z-scan	thf	0.80	[77]
trans,*trans*-[RuCl(dppm)$_2$(-μ-C≡CC$_6$H$_4$-4-C≡C)RuCl(dppm)$_2$]	354	−3200 ± 500	1400 ± 300	3500 ± 600	Z-scan	thf	0.80	[62]
trans,*trans*-[RuCl(dppm)$_2$(-μ-C≡CC$_6$H$_4$-4-C$_6$H$_4$-4-C≡C)RuCl(dppm)$_2$]	360	−1100 ± 300	300 ± 60	1100 ± 300	Z-scan	thf	0.80	[62]
trans,*trans*-[Ru(C≡CPh)(dppe)$_2$(-μ-C≡CC$_6$H$_4$-4-C≡CC≡CC$_6$H$_4$-4-C≡C)-Ru(C≡CPh)(dppe)$_2$]	438	−4000 ± 1500	12000 ± 2000	13000 ± 2400	Z-scan	thf	0.80	[62]
trans-[Ru(C≡CPh)Cl(dppm)$_2$]	308	<120	0	<120	Z-scan	thf	0.80	[48]
trans-[Ru(C≡CC$_6$H$_4$-4-C≡CPh)Cl(dppm)$_2$]	381	65 ± 40	520 ± 200	520 ± 200	Z-scan	thf	0.80	[48]
trans-[Ru(C≡CC$_6$H$_4$-4-CHO)Cl(dppm)$_2$]	405	<120	210 ± 60	210 ± 60	Z-scan	thf	0.80	[48]
trans-[Ru(C≡CC$_6$H$_4$-4-C≡CC$_6$H$_4$-4-NO$_2$)Cl(dppm)$_2$]	464	−160 ± 80	160 ± 60	230 ± 100	Z-scan	thf	0.80	[48]
trans-[Ru(C≡CC$_6$H$_4$-4-C≡CC$_6$H$_4$-4-C≡CC$_6$H$_4$-4-NO$_2$)Cl(dppm)$_2$]	439	−920 ± 200	970 ± 200	1300 ± 300	Z-scan	thf	0.80	[48]
trans-[Ru(C≡CC$_6$H$_4$-4-CHO)Cl(dppe)$_2$]	413	−300 ± 500	<200	−300 ± 500	Z-scan	thf	0.80	[48]
trans-[Ru(C≡CC$_6$H$_4$-4-NO$_2$)Cl(dppe)$_2$]	477	−320 ± 55	<50	−320 ± 55	Z-scan	thf	0.80	[48]
trans-[Ru{C≡CC$_6$H$_4$-4-(*E*)-CH=CHC$_6$H$_4$-4-NO$_2$}Cl(dppe)$_2$]	489	40 ± 200	<100	40 ± 200	Z-scan	thf	0.80	[48]
[Ru(C≡CC$_6$H$_4$-4-CH{OC(O)Me}$_2$)(PPh$_3$)$_2$(η^5-C$_5$H$_5$)]	326	100 ± 100	0	100 ± 100	Z-scan	thf	0.80	[49]
[Ru(C≡CC$_6$H$_4$-4-CHO)(PPh$_3$)$_2$(η^5-C$_5$H$_5$)]	400	−75 ± 50	210 ± 50	220 ± 60	Z-scan	thf	0.80	[49]
trans-[Ru{C≡CC$_6$H$_4$-4-CHO(CHO(CH$_2$)$_3$O }Cl(dppm)$_2$]	320	50 ± 50	0	50 ± 50	Z-scan	thf	0.80	[49]
trans-[Ru(C≡CC$_6$H$_4$-3-CHO)Cl(dppm)$_2$]	321	150 ± 150	0	150 ± 150	Z-scan	thf	0.80	[49]

conformation, and increasing dimensionality can all result in increased cubic nonlinearity. Where applicable, similar trends are seen with the ruthenium acetylide complexes, although in many instances error margins are large (note that many of the small donor–acceptor acetylide complexes were designed for optimizing second-order rather than third-order NLO response). Negative real components of the nonlinearities (γ_{real}) are observed in many instances and significant

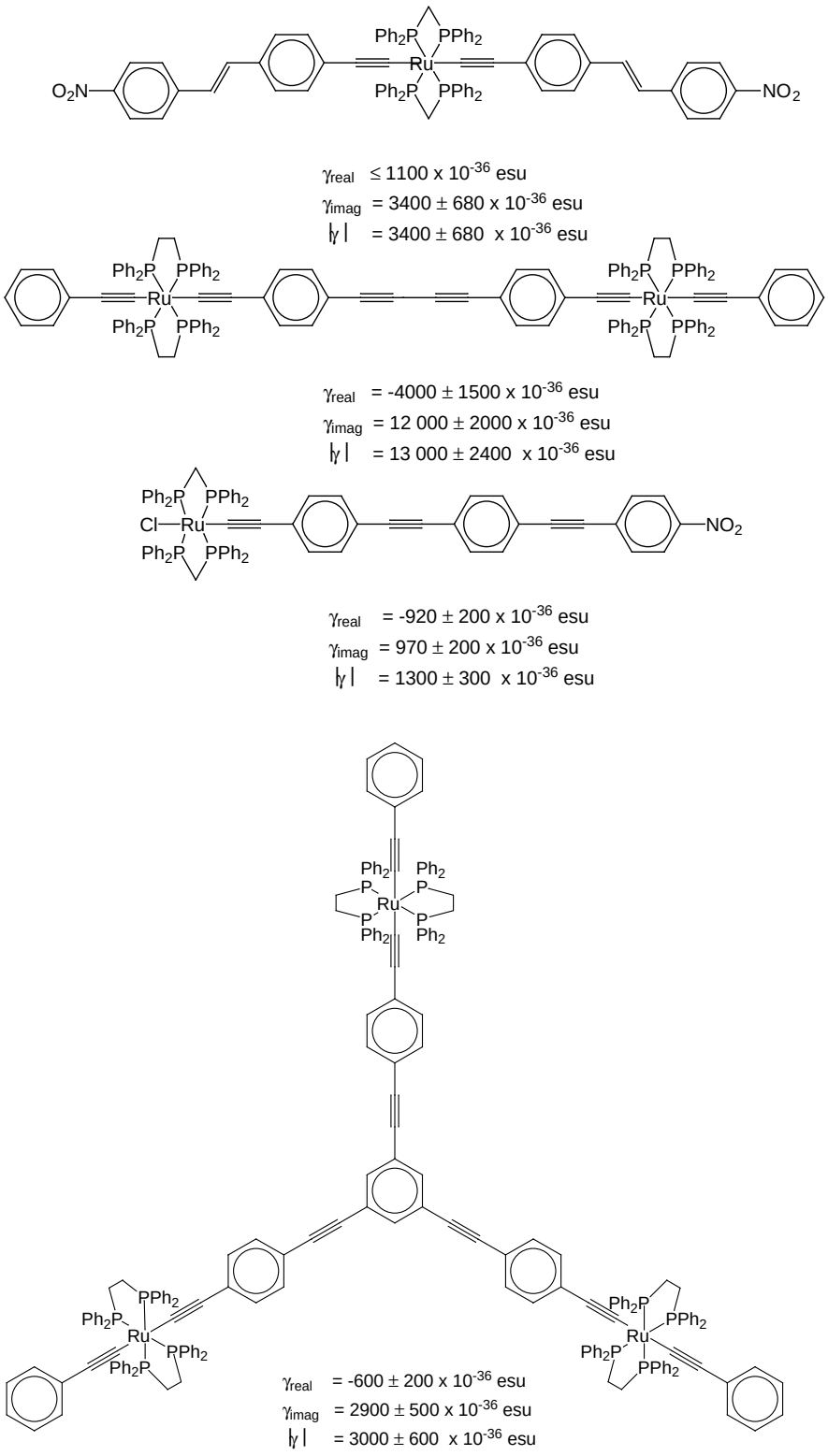

Fig. 12. Group 8 acetylide complexes with large γ values.

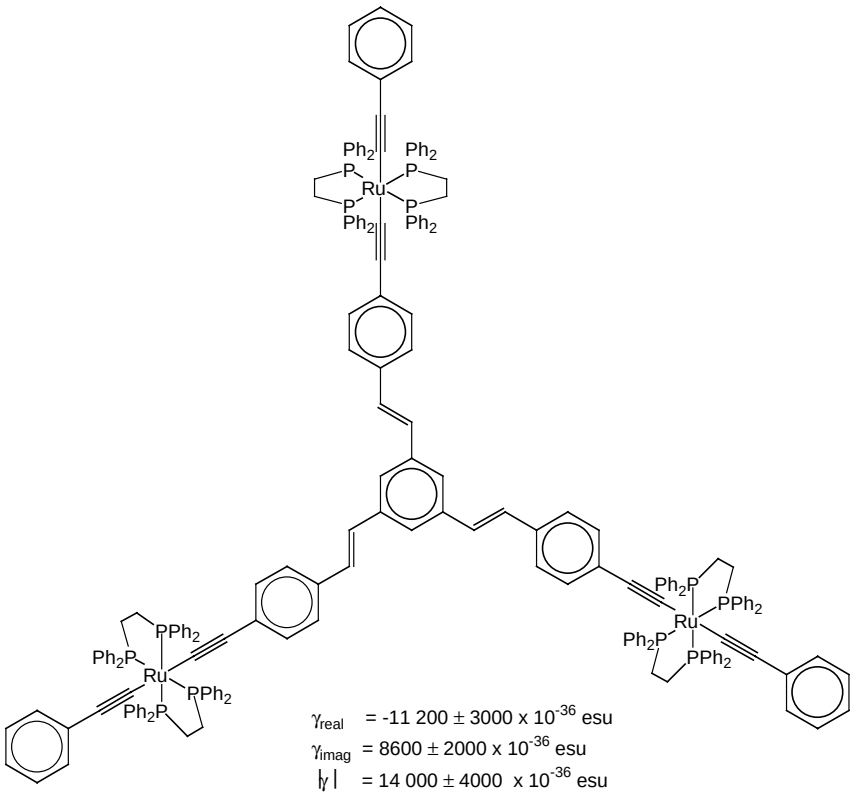

Fig. 12. (*Continued*).

imaginary components (γ_{imag}) are seen for almost all complexes, consistent with two-photon effects contributing to the observed molecular nonlinearities. Two-photon absorption (TPA) is a third-order NLO property that is of interest for applications in multiphoton microscopy, optical limiting, and optical data storage, and for which structure–activity trends are identical with those for γ_{imag}. Cubic nonlinearities for these acetylide complexes increase significantly on progression from monometallic linear ("one-dimensional") complex to bimetallic linear complex, trimetallic octupolar ("two-dimensional") complex [53,54], and nonametallic dendritic complex [74] without significant loss of optical transparency. For these complexes, TPA similarly increases substantially on progression to larger π-delocalizable compounds, TPA cross-sections for the dendritic examples being of the same order of magnitude as the best organic compounds.

5.3. Group 10 acetylide complexes

The molecular cubic nonlinearities of group 10 acetylide complexes for which nonlinearities are reported in cgs units are listed in Table 9, structural formulas of some of the more efficient compounds being shown in Fig. 13. (Cyclopentadienyl)(triphenylphosphine)nickel acetylide complexes were examined by Z-scan at 0.80 μm, the negative γ_{real} and significant γ_{imag} data being suggestive of two-photon dispersion contributing to the observed responses; as noted with the related (cyclopentadienyl)bis(triphenylphosphine)ruthenium complexes, these two-photon states become important for an 800 nm irradiating wavelength when complexes posses $\lambda_{max} > 400$ nm [60]. The γ_{real} values for the nickel complexes are the same (within the error margins) as those of their ruthenium analogues, ease of oxidation and greater delocalization possibilities with the additional triphenylphosphine ligand making no significant difference to cubic NLO merit (in contrast to the situation with quadratic optical nonlinearities).

Cubic nonlinearities for palladium and platinum acetylides have been determined by four-wave mixing or optical Kerr gate techniques, with γ_{real} values uniformly small and γ_{imag} values significant—the data are similar in magnitude to the monoruthenium and nickel acetylide complexes discussed above.

Measurements made by DFWM on group 10 bis(acetylide) complexes for which results have been reported in SI units are listed in Table 10. Although results cannot be directly compared to those mentioned earlier, internal comparisons within the series are valid. These reveal that hyperpolarizability decreases progressing down the group for phenylacetylide and butadiynide complexes. The complexes exhibit a high-order intensity dependence, characteristic of multiphoton resonant enhancement; for these complexes this is possibly due to three-photon resonant enhancement, as λ_{max} is, in all cases, close to 3ω [80–82].

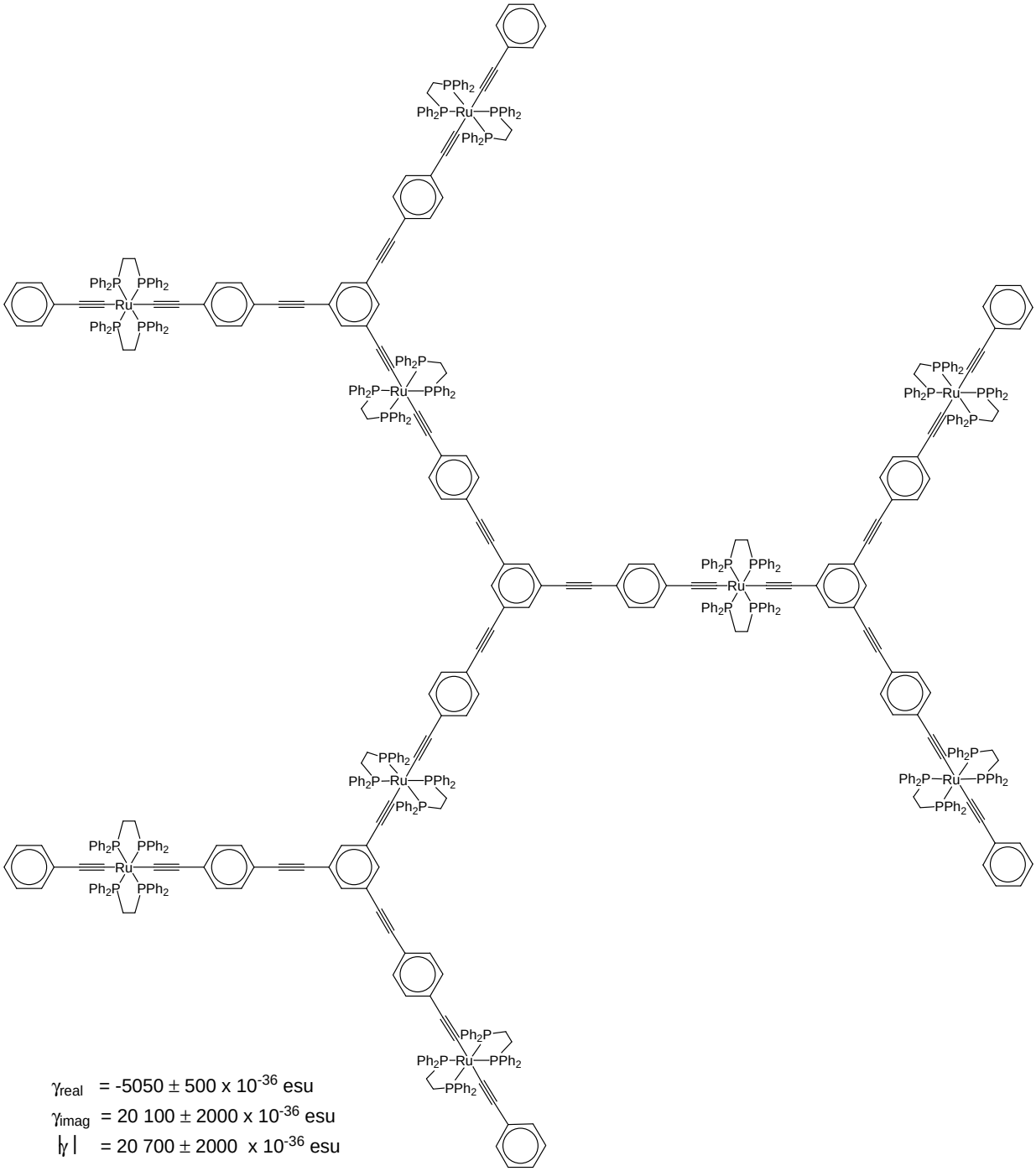

Fig. 12. (*Continued*).

The results for the group 10 acetylide complexes listed in Table 11 have been given as nonlinear refractive indices n_2; once again, these data are available for internal comparison only, because other experimental parameters are needed to derive γ values that are required for comparison to the results given earlier. The results are consistent with increased nonlinearity on chromophore chain lengthening (as observed with acetylide complexes cited earlier) and with a metal efficiency series nickel > platinum > palladium [83].

Many applications in nonlinear optics require materials that are processable, e.g. as thin films, so acetylide polymers are clearly of interest. Group 10 acetylide polymers have proven a fertile area of study. In many of the acetylide polymers of square planar nickel, palladium, and platinum listed in Tables 12 (SI units) and 13 (cgs units), the imaginary part of the nonlinearity is the major contributor, implying significant two-photon absorption. Some of the polymers have nonlinearities that are significantly larger than related

Table 9
Molecular cubic NLO results for group 10 acetylide complexes

Complex	λ_{max} (nm)	γ_{real} (10^{-36} esu)	γ_{imag} (10^{-36} esu)	γ (10^{-36} esu)	Technique	Solvent	Fund. (μm)	Ref.
[Ni(C≡CPh)(PPh$_3$)(η^5-C$_5$H$_5$)]	307	15 ± 10	<10	15 ± 10	Z-scan	thf	0.80	[60]
[Ni(C≡CC$_6$H$_4$-4-NO$_2$)(PPh$_3$)(η^5-C$_5$H$_5$)]	439	−270 ± 100	70 ± 50	280 ± 110	Z-scan	thf	0.80	[60]
[Ni(C≡CC$_6$H$_4$-4-C$_6$H$_4$-4-NO$_2$)(PPh$_3$)(η^5-C$_5$H$_5$)]	413	−580 ± 200	300 ± 60	650 ± 210	Z-scan	thf	0.80	[60]
[Ni(C≡CC$_6$H$_4$-4-(*E*)-CH=CHC$_6$H$_4$-4-NO$_2$)(PPh$_3$)(η^5-C$_5$H$_5$)]	437	−420 ± 100	480 ± 150	640 ± 180	Z-scan	thf	0.80	[60]
[Ni(C≡CC$_6$H$_4$-4-(*Z*)-CH=CHC$_6$H$_4$-4-NO$_2$)(PPh$_3$)(η^5-C$_5$H$_5$)]	417	−230 ± 50	160 ± 80	280 ± 94	Z-scan	thf	0.80	[60]
[Ni(C≡CC$_6$H$_4$-4-C≡CC$_6$H$_4$-4-NO$_2$)(PPh$_3$)(η^5-C$_5$H$_5$)]	417	−640 ± 300	720 ± 300	960 ± 420	Z-scan	thf	0.80	[60]
[Ni(C≡CC$_6$H$_4$-4-N=CHC$_6$H$_4$-4-NO$_2$)(PPh$_3$)(η^5-C$_5$H$_5$)]	448	<120	360 ± 100	360 ± 100	Z-scan	thf	0.80	[60]
trans-[Pd(C≡CPh)$_2$(PBu$^n_3$)$_2$]	[a]			110[b]	FWM	[a]	0.63	[78]
cis,*cis*-[PtCl(PBu$^n_3$)$_2$(-μ-C≡CC$_6$H$_4$-4-C≡C)PtCl(PBu$^n_3$)$_2$]	[a]	11 ± 3	224 ± 56	224 ± 56	OKG/IDA[c]	thf	1.06/0.53	[79]
trans,*trans*-[PtCl(PBu$^n_3$)$_2$(-μ-C≡CC$_6$H$_4$-4-C≡C)PtCl(PBu$^n_3$)$_2$]	[a]	19 ± 5	827 ± 207	827 ± 207	OKG/IDA[c]	thf	1.06/0.53	[79]
trans,*trans*-[PtCl(PBu$^n_3$)$_2$(-μ-C≡CC$_6$H$_4$-4-C≡C)-Pt(PBu$^n_3$)$_2$(-μ-C≡CC$_6$H$_4$-4-C≡C)PtCl(PBu$^n_3$)$_2$]	[a]	45 ± 11	1196 ± 299	1196 ± 299	OKG/IDA[c]	thf	1.06/0.53	[79]
trans,*trans*-[PtCl(PBu$^n_3$)$_2$(-μ-C≡CC$_6$H$_4$-4-C≡CC≡CC$_6$H$_4$-4-C≡C)PtCl(PBu$^n_3$)$_2$]	[a]	88 ± 22	2167 ± 542	2167 ± 542	OKG/IDA[c]	thf	1.06/0.53	[79]
trans-[Pt(C≡CC$_6$H$_4$-4-C≡CH)$_2$(PBu$^n_3$)$_2$]	[a]	53 ± 13	759 ± 190	760 ± 190	OKG/IDA[c]	thf	1.06/0.53	[79]
trans,*trans*-[Pt(C≡CC$_6$H$_4$-4-C≡CH)(PBu$^n_3$)$_2$(-μ-C≡CC$_6$H$_4$-4-C≡C)-Pt(C≡CC$_6$H$_4$-4-C≡CH)(PBu$^n_3$)$_2$]	[a]	66 ± 17	1328 ± 332	1328 ± 332	OKG/IDA[c]	thf	1.06/0.53	[79]
trans,*trans*-[Pt(NCS)(PBu$^n_3$)$_2$(-μ-C≡CC$_6$H$_4$-4-C≡C)Pt(NCS)(PBu$^n_3$)$_2$]	[a]	30 ± 8	1134 ± 284	1134 ± 284	OKG/IDA[c]	thf	1.06/0.53	[79]
trans,*trans*-[PtCl(PBu$^n_3$)$_2$(-μ-C≡CC$_6$H$_4$-4-C≡C)PtCl(PBu$^n_3$)$_2$]	[a]			350[b]	FWM	[a]	0.63	[78]
cis-[Pt(C≡CC$_6$H$_4$-4-C≡CH)$_2$(PBu$^n_3$)$_2$]	[a]	230[b]	260[b]	290[b]	FWM	[a]	0.63	[78]

[a] Not reported.
[b] Error not reported.
[c] IDA, intensity dependent absorption.

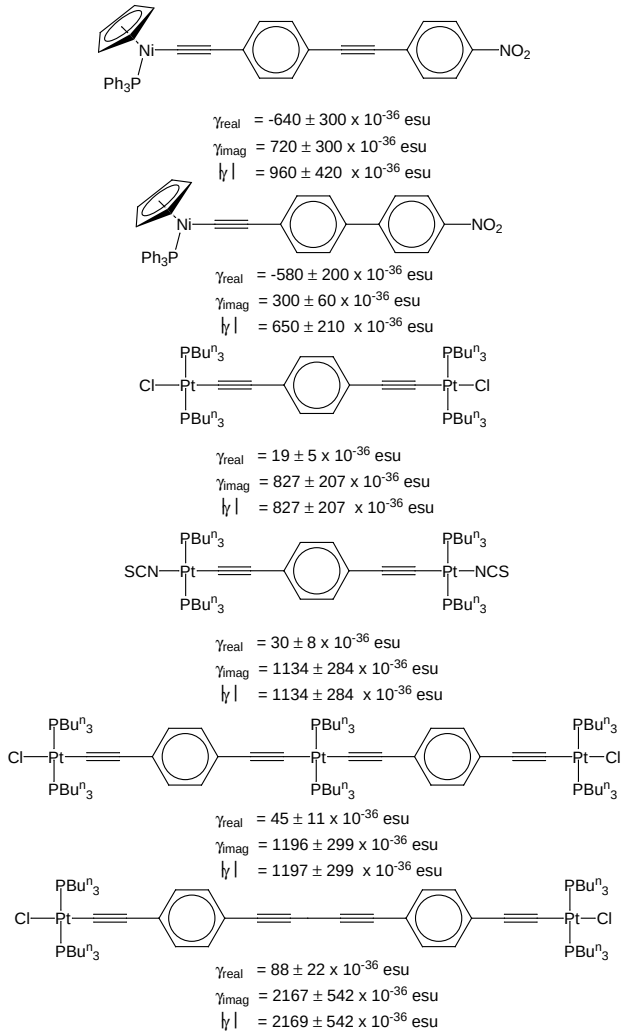

Fig. 13. Group 10 acetylide complexes with large γ values.

monometallic acetylide complexes. There does not seem to be a consistent trend in nonlinearity resultant upon increasing polymer size. Although it is hard to compare data across metal (because the polymers vary in length as well as composition), the platinum polymers are in many cases more efficient than the analogous palladium polymers. The nonlinearities of these polymers do not depend dramatically on aromatic ring substitution, but increasing the number of diethynylarenes in the repeat unit increases the nonlinearity [79,84,85].

Table 11
Nonlinear refractive index measurements for group 10 acetylide complexes[a]

Complex	n_2 (10^{-18} m^2 W^{-1})	Ref.
trans-[Ni(C≡CPh)$_2$(PBu$^n_3$)$_2$]	−16 ± 5	[83]
trans-[Pd(C≡CPh)$_2$(PBu$^n_3$)$_2$]	−0.5 ± 0.1	[83]
trans-[Pd(C≡CC$_6$H$_4$-4-C≡CPh)$_2$(PBu$^n_3$)$_2$]	−25 ± 3	[83]
trans-[Pt(C≡CPh)$_2$(PBu$^n_3$)$_2$]	−3.0 ± 0.1	[83]
trans-[Pt(C≡CC$_6$H$_4$-4-C≡CPh)$_2$(PBu$^n_3$)$_2$]	−209 ± 27	[83]

[a] Z-scan, thf, 0.53 μm.

5.4. Group 11 acetylide complexes

Most of the group 11 acetylide complexes to have been examined thus far are gold complexes, probed by Z-scan at 0.80 μm; the results of these studies are collected in Table 14, with structural formulas of some of the more efficient examples being displayed in Fig. 14. Cubic nonlinearities for many of these 14 electron gold complexes are larger than those of their 18 electron ruthenium analogues, the opposite trend to that observed with β [89]. Replacing PMe_3 by PPh_3 and extending the acetylide ligand both increase π-delocalization possibilities and both result in an increase in $|\gamma|$ values. Introduction of polarizing nitro substituent has a similar effect, but progression from the most efficient monometallic complexes to the iron-digold complexes [Fe{η^5-C$_5$H$_4$-(*E*)-CH=CHC$_6$H$_4$-4-C≡CAu(L)}$_2$] (L = PMe_3, PPh_3, PCy_3) does not result in significant further increase in $|\gamma|$ [77].

Three silver phenylacetylide complexes were examined by heterodyned optical Kerr gate (OHD–OKE) measurements; the data for polymeric compounds are presented in Table 15 ([Ag(C≡CPh)(PPh$_3$)]$_4$ exhibited negligible third-order nonlinearity). The nonlinear responses are in the femtosecond domain and follow the trend silver phenylacetylide polymer > silver phenylacetylide-silver *tert*-butylthiolate double salt > (triphenylphosphine)silver phenylacetylide tetramer [91]. The cubic nonlinearity for the polymer is the largest for acetylide-containing materials, but the uncertainty over extent of polymerization renders impossible a comparison on a "per monomer" basis with the acetylide molecules tabulated above.

Table 10
Molecular cubic NLO measurements of group 10 acetylide complexes[a]

Complex	λ_{max} (nm)	γ_{real} (10^{-44} m^5 V^{-2})	γ_{imag} (10^{-44} m^5 V^{-2})	γ (10^{-44} m^5 V^{-2})	Ref.
trans-[Ni(C≡CPh)$_2$(PEt$_3$)$_2$]	370	−27.5	14.6	31.1	[80,81]
trans-[Ni(C≡CC≡CH)$_2$(PEt$_3$)$_2$]	336	−7.87	17.2	18.9	[80,81]
trans-[Pd(C≡CPh)$_2$(PEt$_3$)$_2$]	370	−21.0	3.39	21.3	[80,81]
trans-[Pd(C≡CC≡CH)$_2$(PEt$_3$)$_2$]	290	−3.85	0.919	3.96	[80–82]
trans-[Pt(C≡CPh)$_2$(PEt$_3$)$_2$]	332	−11.2	2.15	11.4	[80,81]
trans-[Pt(C≡CC≡CH)$_2$(PEt$_3$)$_2$]	318	−1.93	0.771	2.08	[80–82]

[a] DFWM, 1.064 μm, $CHCl_3$.

Table 12
Molecular cubic NLO results for group 10 acetylide polymers[a]

Complex	λ_{max} (nm)	γ_{real} (10^{-42} m^5 V^{-2})	γ_{imag} (10^{-42} m^5 V^{-2})	γ (10^{-42} m^5 V^{-2})	Solvent	Ref.
$[Ni(C{\equiv}CC{\equiv}C)(PBu^n_3)_2]_n$	412	−2.63	−2.41	3.57	$CHCl_3$	[80,81,86]
	410	−2.63	−2.41	3.57		[82]
$[Ni(C{\equiv}CC_6H_4\text{-}4\text{-}C{\equiv}C)(PBu^n_3)_2]_n$		−10	20	20	$CHCl_3$	[86]
$[Ni(C{\equiv}CC_6H_4\text{-}4\text{-}C{\equiv}C)(POc^n{}_3)_2]_n$		−40	100	100	$CHCl_3$	[86]
$[Ni(C{\equiv}CC{\equiv}C)\{P(C_8H_{17})_3\}]_n$		−40	30	50	$CHCl_3$	[86]
$[Pd_2(C{\equiv}CC_6H_4\text{-}4\text{-}C{\equiv}C)(\mu\text{-dppm})_2]_n$		−20	20	20	$CHCl_3$	[86]
$[Pt(C{\equiv}CC{\equiv}C)(PBu^n_3)_2]_n$	364	−1.48	1.74	2.28	$CHCl_3$	[80,81,86]
	360	−1.48	1.74	2.28		[82]

[a] 1.06 μm, DFWM.

5.5. Vinylidene complexes

All reports of cubic nonlinearities for vinylidene complexes thus far are of ruthenium complexes assessed by Z-scan at 0.80 μm, the results from which are collected in Table 16. As with many ruthenium acetylide complexes, the real components of the cubic nonlinearities for the aryldiazovinylidene complexes are negative and the imaginary components are significant, suggestive of two-photon absorption contributing to the observed response. The data are consistent with incorporation of nitro substituent resulting in a significant increase in $|\gamma|$, but nonlinearities for the other monometallic vinylidene complexes are uniformly low. In contrast, the two trimetallic vinylidene complexes to be examined thus far display large cubic NLO efficiencies [54,77].

6. Switching optical nonlinearities of acetylide or vinylidene complexes

There has been considerable success achieved with preparing organic, inorganic, and organometallic compounds with large intrinsic nonlinearities. As a result, attention has recently focused on reversibly modulating ("switching") nonlinearities [92], an area of research in which acetylide complexes have considerable potential. A

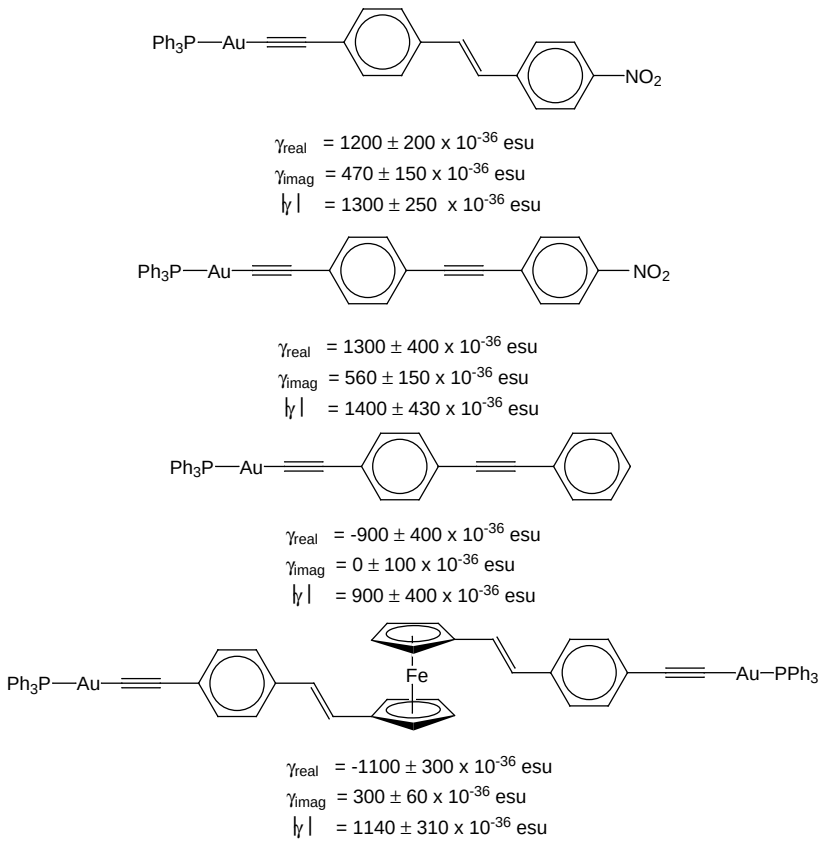

Fig. 14. Gold acetylide complexes with large γ values.

Table 13
Molecular cubic NLO results for group 10 acetylide polymers

Complex	γ_{real} (10^{-36} esu)	γ_{imag} (10^{-36} esu)	γ (10^{-36} esu)	Technique	Solvent	Fund. (μm)	Ref.
[Pd(C≡CC$_6$H$_4$-4-C≡C)(PBu$^n_3$)$_2$]$_n$	390	380	490	FWM		0.63	[78]
[Pd(C≡CC$_6$H$_4$-4-C≡C)(PBu$^n_3$)$_2$]$_n$, n = 112	102	3401		OKG/IDA[a]	thf	1.06/0.53	[84]
[Pd(C≡CC$_6$H$_2$-2,5-Me$_2$-4-C≡C)(PBu$^n_3$)$_2$]$_n$, n = 4	19	1169		OKG/IDA[a]	thf	1.06/0.53	[79]
[Pd(C≡CC$_6$H$_3$-3-NH$_2$-4-C≡C)(PBu$^n_3$)$_2$]$_n$, n = 12	15	1753		OKG/IDA[a]	thf	1.06/0.53	[79]
[Pd(C≡CC$_6$H$_2$-2,5-(OMe)$_2$-4-C≡C)(PBu$^n_3$)$_2$]$_n$, n = 67	22	2432		OKG/IDA[a]	thf	1.06/0.53	[79]
[Pd(C≡CC$_6$H$_4$-4-C≡CC≡CC$_6$H$_4$-4-C≡C)(PBu$^n_3$)$_2$]$_n$ oligomer	66	2094		OKG/IDA[a]	thf	1.06/0.53	[79]
[Pd(C≡CC$_6$H$_2$-2,5-Et$_2$-4-C≡CC≡CC$_6$H$_2$-2,5-Et$_2$-4-C≡C)(PBu$^n_3$)$_2$]$_n$, n = 16	106	3490		OKG/IDA[a]	thf	1.06/0.53	[79]
[Pt(C≡CC$_6$H$_4$-4-C≡C)(PBu$^n_3$)$_2$]$_n$, ~32,000 amu			1470	THG	benzene	1.06	[87]
[Pt(C≡CC$_6$H$_4$-4-C≡C)(PBu$^n_3$)$_2$]$_n$, n = 112	37	1906		OKG/IDA[a]	thf	1.06/0.53	[79]
[Pt(C≡CC$_6$H$_2$-2,5-Me$_2$-4-C≡C)(PBu$^n_3$)$_2$]$_n$, n = 26	29	1200		OKG/IDA[a]	thf	1.06/0.53	[79]
	56	1199		OKG/IDA[a]	thf	1.06/0.53	[88]
[Pt(C≡CC$_6$H$_2$-2,5-Et$_2$-4-C≡C)(PBu$^n_3$)$_2$]$_n$, n = 15	43	956		OKG/IDA[a]	thf	1.06/0.53	[79]
[Pt(C≡CC$_6$H$_3$-3-F-4-C≡C)(PBu$^n_3$)$_2$]$_n$, n = 18	56	1260		OKG/IDA[a]	thf	1.06/0.53	[79]
[Pt(C≡CC$_6$H$_2$-2,5-(OMe)$_2$-4-C≡C)(PBu$^n_3$)$_2$]$_n$, n = 111, 105, 62	48, 65, 43	1724, 1330, 1586		OKG/IDA[a]	thf	1.06/0.53	[79]
[Pt(C≡CC$_6$Me$_4$-4-C≡C)(PBu$^n_3$)$_2$]$_n$ oligomer	28	1324		OKG/IDA[a]	thf	1.06/0.53	[79]
[Pt(C≡CC$_6$H$_3$-3-NH$_2$-4-C≡C)(PBu$^n_3$)$_2$]$_n$, n = 76	18	1342		OKG/IDA[a]	thf	1.06/0.53	[79]
[Pt(C≡CC$_6$H$_3$-3-CF$_3$-4-C≡C)(PBu$^n_3$)$_2$]$_n$, n = 44	34	2148		OKG/IDA[a]	thf	1.06/0.53	[79]
[Pt{C≡C(1-naphthyl)-4-C≡C}(PBu$^n_3$)$_2$]$_n$, n = 62	19	2474		OKG/IDA[a]	thf	1.06/0.53	[79]
[Pt{3-C≡C(C$_5$H$_3$N)-2-C≡C}(PBu$^n_3$)$_2$]$_n$, n = 47, 35	33	2263		OKG/IDA[a]	thf	1.06/0.53	[79]
[Pt(C≡CC$_6$H$_4$-4-C≡C)(PBu$^n_3$)$_2$]$_n$	890	130	1450	FWM		0.63	[78]
[Pt(C≡CC$_6$H$_4$-4-C≡CC≡CC$_6$H$_4$-4-C≡C)(PBu$^n_3$)$_2$]$_n$, n = 223, 97	90, 121	4558, 4025		OKG/IDA[a]	thf	1.06/0.53	[79]
[Pt(C≡CC$_6$H$_4$-4-C≡CC≡CC$_6$H$_4$-4-C≡C)(PBu$^n_3$)$_2$]$_n$, n > 144	856	3570		OKG/IDA[a]	thf	1.06/0.53	[84]
[Pt(C≡CC$_6$H$_2$-2,5-Me$_2$-4-C≡CC≡CC$_6$H$_2$-2,5-Me$_2$-4-C≡C)(PBu$^n_3$)$_2$]$_n$, n = 52, 38	116	2432		OKG/IDA[a]	thf	1.06/0.53	[79]
[Pt(C≡CC$_6$H$_2$-2,5-Me$_2$-4-C≡CC≡CC$_6$H$_2$-2,5-Me$_2$-4-C≡C)(PBu$^n_3$)$_2$]$_n$, n = 52	181	4366		OKG/IDA[a]	thf	1.06/0.53	[84,85]
	120 ± 30	5400 ± 500		OKG	thf	0.53	
[Pt(C≡CC$_6$H$_2$-2,5-Et$_2$-4-C≡CC≡CC$_6$H$_2$-2,5-Et$_2$-4-C≡C)(PBu$^n_3$)$_2$]$_n$, n = 146	79	4933		OKG/IDA[a]	thf	1.06/0.53	[79]
[Pt(C≡CC$_6$H$_4$-4-C≡C)(PBu$^n_3$)$_2$Pt(C≡CC$_6$H$_4$C$_6$H$_4$-4-C≡C)(PBu$^n_3$)$_2$]$_n$, n = 66		4466		OKG/IDA[a]	thf	1.06/0.53	[79]

[a] IDA, intensity dependent absorption.

Table 14
Molecular cubic NLO measurements of gold acetylide complexes[a]

Complex	λ_{max} (nm)	γ_{real} (10^{-36} esu)	γ_{imag} (10^{-36} esu)	γ (10^{-36} esu)	Solvent	Ref.
[Au(C≡CPh)(PPh_3)]	296	39 ± 20	–	39 ± 20	thf	[75]
[Au(C≡CC_6H_4-4-NO_2)(PPh_3)]	338	120 ± 40	20 ± 15	120 ± 40	thf	[75]
[Au(C≡CC_6H_4-4-C_6H_4-4-NO_2)(PPh_3)]	350	540 ± 150	120 ± 50	550 ± 160	thf	[75]
[Au(C≡CC_6H_4-4-(*E*)-CH=CHC_6H_4-4-NO_2)(PPh_3)]	386	1200 ± 200	470 ± 150	1300 ± 250	thf	[75]
[Au(C≡CC_6H_4-4-(*Z*)-CH=CHC_6H_4-4-NO_2)(PPh_3)]	362	420 ± 150	92 ± 30	430 ± 150	thf	[75]
[Au(C≡CC_6H_4-4-C≡CC_6H_4-4-NO_2)(PPh_3)]	362	1300 ± 400	560 ± 150	1400 ± 430	thf	[75]
[Au(C≡CC_6H_4-4-N=CHC_6H_4-4-NO_2)(PPh_3)]	392	130 ± 30	330 ± 60	350 ± 70	thf	[75]
PPN[Au(C≡CC_6H_4-4-NO_2)$_2$]	376	−800 ± 30	115 ± 50	810 ± 60	CH_2Cl_2	[90]
NPr_4[Au(C≡CC_6H_4-4-NO_2)$_2$]	374	90 ± 150	190 ± 50	210 ± 160	CH_2Cl_2	[90]
[Au(C≡CC_6H_4-4-NO_2)($CNBu^t$)]	332	≤130	≤50	≤130	CH_2Cl_2	[90]
[Au(C≡CC_6H_4-4-C_6H_4-4-NO_2)($CNBu^t$)]	343	20 ± 100	70 ± 50	70 ± 110	CH_2Cl_2	[90]
[Au(C≡CC_6H_4-4-(*E*)-CH=CHC_6H_4-4-NO_2)($CNBu^t$)]	381	390 ± 200	1050 ± 300	1120 ± 360	CH_2Cl_2	[90]
[Au(C≡CC_6H_4-4-C_6H_4-4-NO_2){C($NHBu^t$)(NEt_2)}]	354	10 ± 100	160 ± 40	160 ± 110	CH_2Cl_2	[90]
[Au(C≡CC_6H_4-4-(*E*)-CH=CHC_6H_4-4-NO_2){C($NHBu^t$)(NEt_2)}]	389	−200 ± 360	610 ± 200	640 ± 410	CH_2Cl_2	[90]
[Au{C≡CC_6H_4-(*E*)-4-CH=CHPh}(PPh_3)]	338	0 ± 300	0 ± 50	0	thf	[76]
[Au(C≡CC_6H_4-4-C≡CPh)(PPh_3)]	336	−900 ± 400	0 ± 100	900 ± 400	thf	[76]
[Au(C≡CC_6H_4-4-C≡CPh)(PMe_3)]	335	−200 ± 150	0 ± 50	200 ± 150	thf	[76]
[Fe{η^5-C_5H_4-(*E*)-CH=CHC_6H_4-4-C≡CAu(PCy_3)}$_2$]	468	−500 ± 500	500 ± 100	640 ± 390	thf	[77]
[Fe{η^5-C_5H_4-(*E*)-CH=CHC_6H_4-4-C≡CAu(PPh_3)}$_2$]	465	−1100 ± 300	300 ± 60	1140 ± 310	thf	[77]
[Fe{η^5-C_5H_4-(*E*)-CH=CHC_6H_4-4-C≡CAu(PMe_3)}$_2$]	463	200 ± 150	0 ± 30	200 ± 150	thf	[77]
[Au(C≡CC_6H_4-4-NO_2)(PCy_3)]	342	100 ± 50	–	100 ± 50	thf	[62]
[Au(C≡CC_6H_4-4-NO_2)(PPh_3)]	338	120 ± 40	20 ± 15	120 ± 40	thf	[62]
[Au(C≡CC_6H_4-4-NO_2)(PMe_3)]	339	150 ± 50	–	150 ± 50	thf	[62]
[(PCy_3)AuC≡CC_6H_4-4-C≡CAu(PCy_3)]	325	≤250	–	≤250	thf	[62]
[(PCy_3)AuC≡CC_6H_4-4-C_6H_4-4-C≡CAu(PCy_3)]	324	−300 ± 200	0 ± 30	300 ± 200	thf	[62]
[Au(C≡CC_6H_4-4-CHO)(PPh_3)]	322	300 ± 50	0	300 ± 50	thf	[49]
[Au(C≡CC_6H_4-4-CHO)(PMe_3)]	322	35 ± 20	45 ± 30	60 ± 35	thf	[49]
[Au(C≡CC_6H_4-4-$\overline{CHO(CHO(CH_2)_3O}$)($PPh_3$)]	296	−300 ± 200	0 ± 30	300 ± 200	thf	[49]
[Au(C≡CC_6H_4-4-$\overline{CHO(CHO(CH_2)_3O}$)($PMe_3$)]	292	Too low	Too low		thf	[49]
[Au(C≡CC_6H_4-3-CHO)(PPh_3)]	318	Scattered	Scattered		thf	[49]
[Au(C≡CC_6H_4-3-CHO)(PMe_3)]	322	Scattered	Scattered		thf	[49]

[a] Z-scan, 0.80 μm.

variety of approaches to achieve switching have been suggested, with photoisomerization, protonation/deprotonation, and oxidation/reduction the most popular methods of modifying NLO properties. This section provides a summary of attempts to achieve switching with acetylide and vinylidene complexes.

6.1. Switching of quadratic nonlinearities

The results of studies directed at switching quadratic nonlinearities of acetylide or vinylidene complexes are summarized in Table 17, with the most dramatic effect depicted in Fig. 15. While switching via protonation/deprotonation sequences can be effective, the chemical manipulations involved may render this of academic interest only. Many of the vinylidene and acetylide complex pairs in Table 17 have similar nonlinearities, but a five-fold increase in β and β_0 values is observed on deprotonating the vinylidene complex *trans*-[Ru(C=CHC_6H_4-4-(*E*)-CH=CHC_6H_4-4-NO_2)Cl-(dppe)$_2$]PF_6 to afford *trans*-[Ru(C≡CC_6H_4-4-(*E*)-CH=CHC_6H_4-4-NO_2)Cl(dppe)$_2$] [48]. Chemical oxidation and reduction sequences have also been assayed—once again, such chemical manipulations mitigate against possible device applications, but this does afford the opportunity to

Table 15
Molecular and bulk cubic NLO measurements of silver acetylide polymers[a]

Complex	λ_{max} (nm)	$\chi^{(3)}$ (10^{-14} esu)	γ^b (10^{-36} esu)	Solvent	Ref.
[AgC≡CPh]$_n$	260	2.40	90700	1:1 DMSO/$CHCl_3$	[91]
	271	−1.11	−105900	1:1:1 DMSO/$CHCl_3$/CH_2Cl_2	[91]
[AgC≡CPh·AgS(Bu^t)]$_n$	264	1.10	74400	1:1 DMSO/$CHCl_3$	[91]
	271	−0.68	−64900	1:1:1 DMSO/$CHCl_3$/CH_2Cl_2	[91]

[a] Optically heterodyned optical Kerr effect, 0.647 μm.
[b] Calculated with the assumption that $n = 7$.

Table 16
Molecular cubic NLO measurements of vinylidene complexes[a]

Complex	λ_{max} (nm)	γ_{real} (10^{-36} esu)	γ_{imag} (10^{-36} esu)	γ (10^{-36} esu)	Solvent	Ref.
$[Fe\{\eta^5\text{-}C_5H_4\text{-}(E)\text{-}CH{=}CHC_6H_4\text{-}4\text{-}CH{=}CRuCl(dppm)_2\}_2](PF_6)_2$	383	−3000 ± 1200	2300 ± 800	3800 ± 1400	thf	[77]
$[Ru(C{=}CPhN{=}NPh)(PPh_3)_2(\eta^5\text{-}C_5H_5)]BF_4$	363	−160 ± 60	75 ± 25	180 ± 65	CH_2Cl_2	[63]
$[Ru(C{=}CPhN{=}NC_6H_4\text{-}2\text{-}OMe)(PPh_3)_2(\eta^5\text{-}C_5H_5)]Cl$	377	−220 ± 150	70 ± 30	230 ± 150	CH_2Cl_2	[63]
$[Ru(C{=}CPhN{=}NC_6H_4\text{-}3\text{-}OMe)(PPh_3)_2(\eta^5\text{-}C_5H_5)]BF_4$	389	−310 ± 60	90 ± 30	320 ± 65	CH_2Cl_2	[63]
$[Ru(C{=}CPhN{=}NC_6H_4\text{-}4\text{-}OMe)(PPh_3)_2(\eta^5\text{-}C_5H_5)]Cl$	374	−20 ± 40	80 ± 40	80 ± 50	CH_2Cl_2	[63]
$[Ru(C{=}CPhN{=}NC_6H_4\text{-}4\text{-}NO_2)(PPh_3)_2(\eta^5\text{-}C_5H_5)]BF_4$	413	−320 ± 100	160 ± 40	360 ± 110	CH_2Cl_2	[63]
$[Ru(C{=}CPhN{=}NC_6H_4\text{-}4\text{-}NO_2)(PPh_3)_2(\eta^5\text{-}C_5H_5)]Cl$	413	−630 ± 200	160 ± 50	650 ± 210	CH_2Cl_2	[63]
$[Ru(C{=}CPhN{=}NC_6H_4\text{-}4\text{-}NO_2)(PPh_3)_2(\eta^5\text{-}C_5H_5)]Br$	413	−570 ± 150	150 ± 40	590 ± 160	CH_2Cl_2	[63]
$[Ru(C{=}CPhN{=}NC_6H_4\text{-}4\text{-}NO_2)(PPh_3)_2(\eta^5\text{-}C_5H_5)]I$	413	−460 ± 50	140 ± 50	480 ± 60	CH_2Cl_2	[63]
$[Ru(C{=}CPhN{=}NC_6H_4\text{-}4\text{-}NO_2)(PPh_3)_2(\eta^5\text{-}C_5H_5)](4\text{-}MeC_6H_4SO_3)$	413	−580 ± 200	210 ± 50	620 ± 210	CH_2Cl_2	[63]
$[Ru(C{=}CPhN{=}NC_6H_4\text{-}4\text{-}NO_2)(PPh_3)_2(\eta^5\text{-}C_5H_5)]NO_3$	413	−460 ± 150	200 ± 50	500 ± 160	CH_2Cl_2	[63]
trans-$[Ru(C{=}CHPh)Cl(dppm)_2]PF_6$	320	<440	<50	<440	thf	[48]
trans-$[Ru(C{=}CHC_6H_4\text{-}4\text{-}C{\equiv}CPh)Cl(dppm)_2]PF_6$	380	<500	0	<500	thf	[48]
trans-$[Ru(C{=}CHC_6H_4\text{-}4\text{-}CHO)Cl(dppm)_2]PF_6$	403	0	<20	<20	thf	[48]
trans-$[Ru(C{=}CHC_6H_4\text{-}4\text{-}NO_2)Cl(dppm)_2]PF_6$	470	<50	<30	<50	thf	[48]
trans-$[Ru(C{=}CHC_6H_4\text{-}4\text{-}C{\equiv}CC_6H_4\text{-}4\text{-}NO_2)Cl(dppm)_2]PF_6$	326	<500	420 ± 60	420 ± 60	thf	[48]
trans-$[Ru(C{=}CHPh)Cl(dppe)_2]PF_6$	317	380 ± 400	<50	380 ± 400	thf	[48]
trans-$[Ru(C{=}CHC_6H_4\text{-}4\text{-}CHO)Cl(dppe)_2]PF_6$	412	<260	0	<260	thf	[48]
trans-$[Ru(C{=}CHC_6H_4\text{-}4\text{-}NO_2)Cl(dppm)_2]PF_6$	476	250 ± 300	<50	250 ± 300	thf	[48]
trans-$[Ru\{C{=}CHC_6H_4\text{-}4\text{-}(E)\text{-}CH{=}CHC_6H_4\text{-}4\text{-}NO_2\}Cl(dppe)_2]PF_6$	473	650 ± 500	<50	650 ± 500	thf	[48]
trans-$[Ru\{C{=}CHC_6H_4\text{-}4\text{-}\overbrace{CHO(CHO(CH_2)_3O}\}Cl(dppm)_2]PF_6$	317	75 ± 75	0	75 ± 75	thf	[49]
trans-$[Ru(C{=}CHC_6H_4\text{-}3\text{-}CHO)Cl(dppm)_2]PF_6$	320	200 ± 200	0	200 ± 200	thf	[49]
trans-$[Ru(C{=}CHC_6H_4\text{-}4\text{-}CHO)Cl(dppm)_2]PF_6$	403	0	<20	<20	thf	[49]
[1,3,5-*trans*-$[RuCl(dppm)_2\{C{=}CHC_6H_4\text{-}(E)\text{-}4\text{-}CH{=}CH\}_3C_6H_3](PF_6)_3$	396	−900 ± 500	700 ± 400	1100 ± 700	thf	[54]

[a] Z-scan, 0.800 μm.

Table 17
Switching of molecular quadratic NLO properties[a]

Complex	λ (nm)	β (10^{-30} esu)	β_0 (10^{-30} esu)	Switch	Solvent	Ref.
$[1,3\text{-}C_6H_4\{(C{\equiv}C)Fe(dppe)(\eta^5\text{-}C_5Me_5)\}_2]$	349	210	98		CH_2Cl_2	[52]
$[1,3\text{-}C_6H_4\{(C{\equiv}C)Fe(dppe)(\eta^5\text{-}C_5Me_5)\}_2]PF_6$	650	150	21	Chem. oxid.	CH_2Cl_2	[52]
$[1,3\text{-}C_6H_4\{(C{\equiv}C)Fe(dppe)(\eta^5\text{-}C_5Me_5)\}_2](PF_6)_2$	662	200	30	Chem. oxid.	CH_2Cl_2	[52]
$[1,3,5\text{-}C_6H_3\{(C{\equiv}C)Fe(dppe)(\eta^5\text{-}C_5Me_5)\}_3]$	351	175	87		CH_2Cl_2	[52]
$[1,3,5\text{-}C_6H_3\{(C{\equiv}C)Fe(dppe)(\eta^5\text{-}C_5Me_5)\}_3]PF_6$	710	190	35	Chem. oxid.	CH_2Cl_2	[52]
$[1,3,5\text{-}C_6H_3\{(C{\equiv}C)Fe(dppe)(\eta^5\text{-}C_5Me_5)\}_3](PF_6)_2$	688	170	29	Chem. oxid.	CH_2Cl_2	[52]
$[1,3,5\text{-}C_6H_3\{(C{\equiv}C)Fe(dppe)(\eta^5\text{-}C_5Me_5)\}_3](PF_6)_3$	662	53	8	Chem. oxid.	CH_2Cl_2	[52]
$[1,4\text{-}C_6H_4\{(C{\equiv}C)Fe(dppe)(\eta^5\text{-}C_5Me_5)\}_2]$	413	180	60		CH_2Cl_2	[52]
$[1,4\text{-}C_6H_4\{(C{\equiv}C)Fe(dppe)(\eta^5\text{-}C_5Me_5)\}_2]PF_6$	702	400	72	Chem. oxid.	CH_2Cl_2	[52]
$[1,4\text{-}C_6H_4\{(C{\equiv}C)Fe(dppe)(\eta^5\text{-}C_5Me_5)\}_2](PF_6)_2$	702	200	36	Chem. oxid.	CH_2Cl_2	[52]
trans-$[Ru(C{\equiv}CPh)Cl(dppm)_2]$	308	20	12		thf	[41]
trans-$[Ru(C{=}CHPh)Cl(dppm)_2]PF_6$	320	24	16	$+H^+$	thf	[48]
trans-$[Ru(C{\equiv}CPh)Cl(dppe)_2]$	319	6	3		thf	[48]
trans-$[Ru(C{=}CHPh)Cl(dppe)_2]PF_6$	317	[b]	[b]	$+H^+$	thf	[48]
trans-$[Ru(C{\equiv}CC_6H_4\text{-}4\text{-}C{\equiv}CPh)Cl(dppm)_2]$	381	101	43		thf	[48]
trans-$[Ru(C{=}CHC_6H_4\text{-}4\text{-}C{\equiv}CPh)Cl(dppm)_2]PF_6$	380	64	31	$+H^+$	thf	[48]
trans-$[Ru(C{\equiv}CC_6H_4\text{-}4\text{-}CHO)Cl(dppm)_2]$	405	106	38		thf	[48]
trans-$[Ru(C{=}CHC_6H_4\text{-}4\text{-}CHO)Cl(dppm)_2]PF_6$	403	108	39	$+H^+$	thf	[48]
trans-$[Ru(C{\equiv}CC_6H_4\text{-}4\text{-}CHO)Cl(dppe)_2]$	413	120	40		thf	[48]
trans-$[Ru(C{=}CHC_6H_4\text{-}4\text{-}CHO)Cl(dppe)_2]PF_6$	412	181	61	$+H^+$	thf	[48]
trans-$[Ru(C{\equiv}CC_6H_4\text{-}4\text{-}NO_2)Cl(dppm)_2]$	473	767	129		thf	[41]
trans-$[Ru(C{=}CHC_6H_4\text{-}4\text{-}NO_2)Cl(dppm)_2]PF_6$	470	721	127	$+H^+$	thf	[48]
trans-$[Ru(C{\equiv}CC_6H_4\text{-}4\text{-}NO_2)Cl(dppe)_2]$	477	351	55		thf	[48]
trans-$[Ru(C{=}CHC_6H_4\text{-}4\text{-}NO_2)Cl(dppe)_2]PF_6$	476	1130	180	$+H^+$	thf	[48]

Table 17 (*Continued*)

Complex	λ (nm)	β (10^{-30} esu)	β_0 (10^{-30} esu)	Switch	Solvent	Ref.
trans-[Ru(C≡CC_6H_4-4-C≡CC_6H_4-4-NO_2)Cl(dppm)$_2$]	464	833	161		thf	[48]
trans-[Ru(C=CHC_6H_4-4-C≡CC_6H_4-4-NO_2)Cl(dppm)$_2$]PF_6	326	424	122	$+H^+$	thf	[48]
trans-[Ru(C≡CC_6H_4-4-(*E*)-CH=CHC_6H_4-4-NO_2)Cl(dppm)$_2$]	490	1964	235		thf	[41]
trans-[Ru(C=CHC_6H_4-4-(*E*)-CH=CHC_6H_4-4-NO_2)Cl(dppm)$_2$]PF_6	369	1899	314	$+H^+$	thf	[48]
trans-[Ru(C≡CC_6H_4-4-(*E*)-CH=CHC_6H_4-4-NO_2)Cl(dppe)$_2$]	489	2676	342		thf	[48]
trans-[Ru(C=CHC_6H_4-4-(*E*)-CH=CHC_6H_4-4-NO_2)Cl(dppe)$_2$]PF_6	473	441	74	$+H^+$	thf	[48]

[a] HRS, 1.064 μm.
[b] Scatters.

access more than two NLO "states" in a system. For example, stepwise oxidation of [1,3,5-C_6H_3{(C≡C)Fe(dppe)-(η^5-C_5Me_5)}$_3$] affords, in a stepwise fashion, $Fe^{II}Fe^{II}Fe^{II}$, $Fe^{II}Fe^{II}Fe^{III}$, $Fe^{II}Fe^{III}Fe^{III}$, and finally $Fe^{III}Fe^{III}Fe^{III}$ complexes, with a three-fold difference in β value the largest variation across these states [52].

6.2. Switching of cubic nonlinearities

Studies aimed at switching cubic nonlinearities are summarized in Table 18, with an example illustrated in Fig. 16. Attempts thus far have used protonation/deprotonation and redox methods. The low nonlinearities and significant error margins frustrated most attempts to demonstrate switching with vinylidene/acetylide complex pairs—perhaps the most clear-cut example afforded a five-fold increase in γ value on proceeding from *trans*-[Ru(C=CHC_6H_4-4-NO_2)Cl-(dppm)$_2$]PF_6 to *trans*-[Ru(C≡CC_6H_4-4-NO_2)Cl(dppm)$_2$] [48,68].

Facile switching using an optically-transparent thin-layer electrochemical cell has recently been demonstrated [93,94], a procedure that avoids the chemical transformations remote

Table 18
Switching of molecular cubic NLO properties[a]

Complex	λ (nm)	γ_{real} (10^{-36} esu)	γ_{imag} (10^{-36} esu)	γ (10^{-36} esu)	Switch	Solvent	Ref.
trans-[Ru(C≡CPh)Cl(dppm)$_2$]	308	<120	0	<120		thf	[48]
trans-[Ru(C=CHPh)Cl(dppm)$_2$]PF_6	320	<440	<50	<440	$+H^+$	thf	[48]
trans-[Ru(C≡CPh)Cl(dppe)$_2$]	319	−170 ± 40	71 ± 20	180 ± 45		CH_2Cl_2	[11]
trans-[Ru(C=CHPh)Cl(dppe)$_2$]PF_6	317	380 ± 400	<50	380 ± 400	$+H^+$	thf	[48]
trans-[Ru(C≡CC_6H_4-4-C≡CPh)Cl(dppm)$_2$]	381	65 ± 40	520 ± 200	520 ± 200		thf	[48]
trans-[Ru(C=CHC_6H_4-4-C≡CPh)Cl(dppm)$_2$]PF_6	380	<500	0	<500	$+H^+$	thf	[48]
trans-[Ru(C≡CC_6H_4-4-CHO)Cl(dppm)$_2$]	405	<120	210 ± 60	210 ± 60		thf	[48]
trans-[Ru(C=CHC_6H_4-4-CHO)Cl(dppm)$_2$]PF_6	403	0	<20	<20	$+H^+$	thf	[48]
trans-[Ru(C≡CC_6H_4-4-CHO)Cl(dppe)$_2$]	413	−300 ± 500	<200	300 ± 500		thf	[48]
trans-[Ru(C=CHC_6H_4-4-CHO)Cl(dppe)$_2$]PF_6	412	<260	0	<260	$+H^+$	thf	[48]
trans-[Ru(C≡CC_6H_4-4-NO_2)Cl(dppm)$_2$]	473	170 ± 34	230 ± 46	290 ± 60		CH_2Cl_2	[68]
trans-[Ru(C=CHC_6H_4-4-NO_2)Cl(dppm)$_2$]PF_6	470	<50	<30	<50	$+H^+$	thf	[48]
trans-[Ru(C≡CC_6H_4-4-NO_2)Cl(dppe)$_2$]	477	320 ± 55	<50	320 ± 55		thf	[48]
trans-[Ru(C=CHC_6H_4-4-NO_2)Cl(dppe)$_2$]PF_6	476	250 ± 300	<50	250 ± 300	$+H^+$	thf	[48]
trans-[Ru(C≡CC_6H_4-4-C≡CC_6H_4-4-NO_2)Cl(dppm)$_2$]	464	−160 ± 80	160 ± 60	230 ± 100		thf	[48]
trans-[Ru(C=CHC_6H_4-4-C≡CC_6H_4-4-NO_2)Cl(dppm)$_2$]PF_6	326	<500	420 ± 60	420 ± 60	+H+	thf	[48]
trans-[Ru(C≡CC_6H_4-4-(*E*)-CH=CHC_6H_4-4-NO_2)Cl(dppm)$_2$]	490	200 ± 40	1100 ± 220	1100 ± 220		CH_2Cl_2	[68]
trans-[Ru(C=CHC_6H_4-4-(*E*)-CH=CHC_6H_4-4-NO_2)Cl(dppm)$_2$]PF_6	369	[b]	[b]	[b]	$+H^+$	thf	[48]
trans-[Ru(C≡CC_6H_4-4-(*E*)-CH=CHC_6H_4-4-NO_2)Cl(dppe)$_2$]	489	40 ± 200	<100	40 ± 200		thf	[48]
trans-[Ru(C=CHC_6H_4-4-(*E*)-CH=CHC_6H_4-4-NO_2)Cl(dppe)$_2$]PF_6	473	650 ± 500	<50	650 ± 500	$+H^+$	thf	[48]
trans-[Ru(C≡CPh)Cl(dppm)$_2$]	318	<300	<200	<300		CH_2Cl_2	[93,94]
trans-[Ru(C≡CPh)Cl(dppm)$_2$]$^+$	833	1300 ± 500	−2200 ± 1000	2600 ± 1000	echem	CH_2Cl_2	[93,94]
trans-[Ru(C≡CC_6H_4-4-C≡CPh)Cl(dppe)$_2$]	388	−100 ± 100	450 ± 200	460 ± 200		CH_2Cl_2	[93,94]
trans-[Ru(C≡CC_6H_4-4-C≡CPh)Cl(dppe)$_2$]$^+$	893	2900 ± 1000	−1200 ± 600	3100 ± 1000	echem	CH_2Cl_2	[93,94]
[1,3,5-[*trans*-[RuCl(dppe)$_2$(C≡CC_6H_4C≡C)]$_3$(C_6H_3)]	413	−330 ± 100	2200 ± 500	2200 ± 600		CH_2Cl_2	[93,94]
[1,3,5-{*trans*-RuCl(dppe)$_2$(C≡CC_6H_4C≡C)}$_3$(C_6H_3)]$^{3+}$	893	13500 ± 3000	−4700 ± 500	14000 ± 3000	echem	CH_2Cl_2	[93,94]

[a] Z-scan, 0.80 μm.
[b] Scatters.

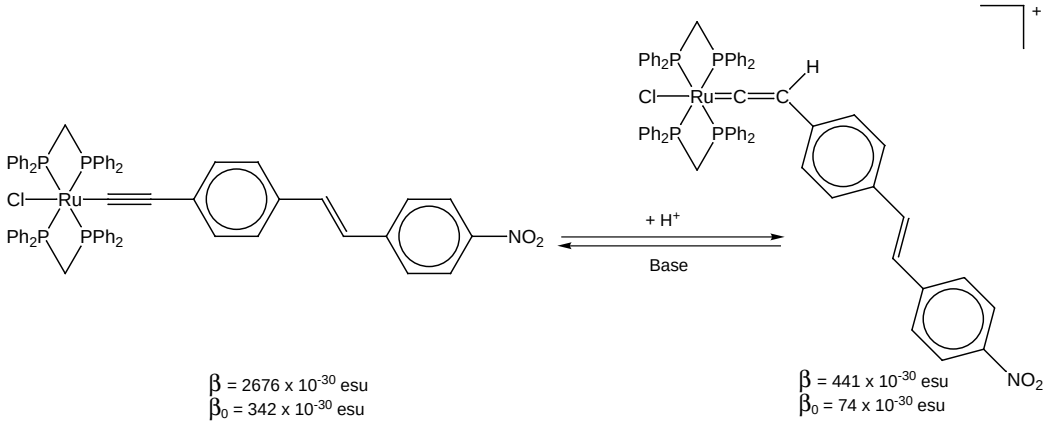

Fig. 15. Example of switching quadratic NLO response by a protonation/deprotonation sequence.

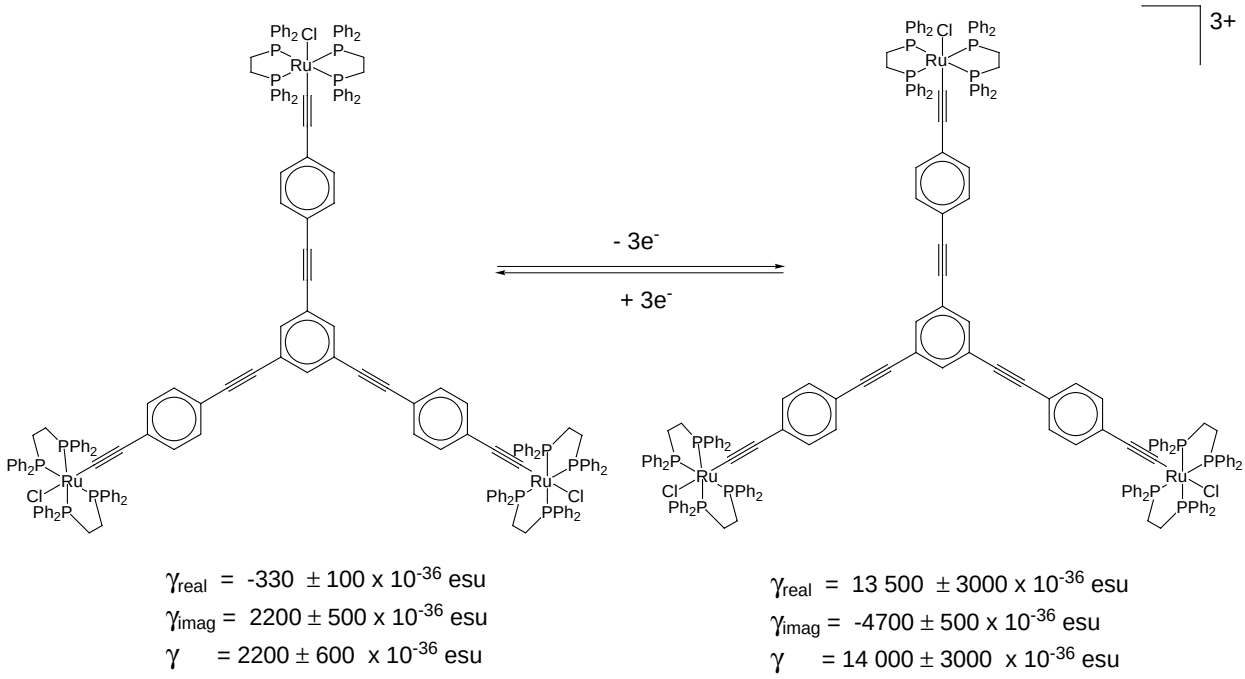

Fig. 16. Example of switching cubic NLO response by an oxidation/reduction sequence.

from the optical bench employed in other studies. The complexes *trans*-[Ru(C≡CPh)Cl(dppm)$_2$], *trans*-[Ru(C≡CC$_6$H$_4$-4-C≡CPh)Cl(dppe)$_2$], and [1,3,5-[*trans*-[RuCl-(dppe)$_2$(C≡CC$_6$H$_4$-4-C≡C)]$_3$(C$_6$H$_3$)] are transparent at wavelengths >500 nm, but following oxidation the resultant cationic complexes have strong absorption bands at long wavelength with appreciable intensity at the fundamental wavelength of a Ti-sapphire laser (800 nm). The nonlinearity of the first-named complex was too low to measure at 800 nm, and the other two complexes are significant two-photon absorbers at this wavelength, but the strong one-photon absorption conditions in the oxidized form result in all three complex cations being saturable absorbers. The first-named complex therefore has third-order nonlinearity "switched on" upon oxidation, while the other two complexes have the sign and magnitude of γ_{real} and γ_{imag} changed upon oxidation. This electrochemical switching in solution is diffusion controlled, the ca. 5 min required for each complete oxidation or reduction process mitigating against applications.

7. Conclusions

The studies of the NLO properties of acetylide and vinylidene complexes summarized above have resulted in development of structure–NLO response relationships for quadratic optical nonlinearities, while low nonlinearities and large error margins for many of the studies with small acetylide complexes have resulted in less success at developing relationships for cubic nonlinearities. To illustrate the optimum combination of metal and ligands, Tables 19 and 20 collect

Table 19
Quadratic NLO-efficient molecules by metal[a]

Complex	λ_{max} (nm)	β (10^{-30} esu)	β_0 (10^{-30} esu)	Ref.
[Fe(C≡CC$_6$H$_4$-4-NO$_2$)(dppe)(η^5-C$_5$H$_5$)]	498	665	64	[50]
$(-)_{589}$-*trans*-[Ru(C≡CC$_6$H$_4$-4-(*E*)-CH=CHC$_6$H$_4$-4-NO$_2$)Cl{(*R*,*R*)-diph}$_2$]	481	2795	406	[55]
[Os(C≡CC$_6$H$_4$-4-NO$_2$)(PPh$_3$)$_2$(η^5-C$_5$H$_5$)]	474	1051	174	[50]
[Ni(C≡CC$_6$H$_4$-4-(*E*)-CH=CHC$_6$H$_4$-4-NO$_2$)(PPh$_3$)(η^5-C$_5$H$_5$)]	437	445	120	[60]
[Au(C≡CC$_6$H$_4$-4-(*E*)-N=NC$_6$H$_4$-4-NO$_2$)(PPh$_3$)]	398	180	68	[45]

[a] HRS, thf solvent, 1.064 μm.

Table 20
Cubic NLO-efficient molecules by metal[a]

Complex	λ_{max} (nm)	γ_{real} (10^{-36} esu)	γ_{imag} (10^{-36} esu)	γ (10^{-36} esu)	Ref.
[Fe(C≡CC$_6$H$_4$-4-(*E*)-CH=CHC$_6$H$_4$-4-NO$_2$)(dppe)(η^5-C$_5$H$_5$)]	499	−2200 ± 600	1200 ± 300	2500 ± 670	[95]
1,3,5-C$_6$H$_3$-(C≡CC$_6$H$_4$-4-C≡C-*trans*-[Ru(dppe)$_2$]C≡C-3,5-C$_6$H$_3$-{C≡CC$_6$H$_4$-4-C≡C-*trans*-[Ru(C≡CPh)(dppe)$_2$]}$_2$)$_3$	402	−5050 ± 500	20100 ± 2000	20700 ± 2000	[74]
[Ni(C≡CC$_6$H$_4$-4-C≡CC$_6$H$_4$-4-NO$_2$)(PPh$_3$)(η^5-C$_5$H$_5$)]	417	−640 ± 300	720 ± 300	960 ± 420	[60]
[Au(C≡CC$_6$H$_4$-4-C≡CC$_6$H$_4$-4-NO$_2$)(PPh$_3$)]	362	1300 ± 400	560 ± 150	1400 ± 430	[75]

[a] Z-scan, thf solvent, 0.80 μm.

data for the most efficient molecules for each metal (because of the aforementioned difficulty in comparing results from differing laboratories and using different techniques, data from the most active laboratory and standard conditions have been tabulated).

Some of the acetylide complexes are amongst the most efficient organic or inorganic quadratic NLO molecules thus far, while the ruthenium acetylide dendrimers possess two-photon absorption cross-sections of the same order of magnitude as the best organic performers. The recent progress with switching the quadratic and cubic nonlinearity of acetylide complexes using oxidation/reduction processes is an area in which these complexes may well prove superior to organic molecules, due to the readily available oxidation states of the acetylide complexes. This area is likely to undergo further development in the near future.

References

[1] D.S. Chemla, J. Zyss (Eds.), Nonlinear Optical Properties of Organic Molecules and Crystals II, Academic Press, Orlando, 1987.
[2] D.S. Chemla, J. Zyss (Eds.), Nonlinear Optical Properties of Organic Molecules and Crystals I, Academic Press, Orlando, 1987.
[3] D.J. Williams (Ed.), Nonlinear Optical Properties of Organic and Polymeric Materials, American Chemical Society, Washington, DC, 1983.
[4] B. Kirtman, B. Champagne, Int. Rev. Phys. Chem. 16 (1997) 389.
[5] R.A. Hann, D. Bloor (Eds.), Organic Materials for Non-Linear Optics, Royal Society of Chemistry, London, 1989.
[6] R.A. Hann, D. Bloor (Eds.), Organic Materials for Non-linear Optics II, Royal Society of Chemistry, London, 1991.
[7] T. Verbiest, S. Houbrechts, M. Kauranen, K. Clays, A. Persoons, J. Mater. Chem. 7 (1997) 2175.
[8] N.J. Long, Angew. Chem. Int. Ed. Engl. 34 (1995) 21.
[9] S. Di Bella, Chem. Soc. Rev. 30 (2001) 355.
[10] I.R. Whittall, A.M. McDonagh, M.G. Humphrey, M. Samoc, Adv. Organomet. Chem. 42 (1998) 291.
[11] I.R. Whittall, A.M. McDonagh, M.G. Humphrey, M. Samoc, Adv. Organomet. Chem. 43 (1999) 349.
[12] S.R. Marder, in: D.W. Bruce, D. O'Hare (Eds.), Inorganic Materials, Wiley, Chichester, 1992, p. 116.
[13] W. Nie, Adv. Mater. 5 (1993) 520.
[14] S. Allen, New Scientist 1 July (1989) 31.
[15] A.J. Heeger, J. Orenstein, D. Ulrich (Eds.), Nonlinear Optical Properties of Polymers, Materials Research Society, Pittsburgh, 1988.
[16] G.J. Ashwell, D. Bloor (Eds.), Organic Materials for Non-linear Optics III, Royal Society of Chemistry, Cambridge, 1993.
[17] J. Messier, F. Kajzar, P. Prasad, D. Ulrich (Eds.), Nonlinear Optical Effects in Organic Polymers, Kluwer Academic Publishers, Dordrecht, 1989.
[18] J. Messier, F. Kajzar, P. Prasad (Eds.), Organic Molecules for Nonlinear Optics and Photonics, Kluwer Academic Publishers, Dordrecht, 1991.
[19] T. Kobayashi (Ed.), Nonlinear Optics of Organics and Semiconductors, Springer-Verlag, Berlin, 1989.
[20] M.H. Lyons (Ed.), Materials for Non-Linear and Electro-Optics 1989, Institute of Physics, Bristol, 1989.
[21] S.R. Marder, J.E. Sohn, G.D. Stucky (Eds.), Materials for Nonlinear Optics, Chemical Perspectives, American Chemical Society, Washington, DC, 1991.
[22] D.J. Williams, Angew. Chem. Int. Ed. 23 (1984) 690.
[23] H.S. Nalwa, Adv. Mater. 5 (1993) 341.
[24] H.S. Nalwa, Appl. Organomet. Chem. 5 (1991) 1.
[25] H.S. Nalwa, T. Watanabe, S. Miyata, Adv. Mater. 7 (1995) 754.
[26] D.R. Kanis, M.A. Ratner, T.J. Marks, Chem. Rev. 94 (1994) 195.
[27] R. Nast, Angew. Chem. Int. Ed. 72 (1960) 26.
[28] M.G. Humphrey, J. Organomet. Chem. 670 (2003) 1.
[29] N.J. Long, C.K. Williams, Angew. Chem. Int. Ed. 42 (2003) 2586.
[30] R.W. Boyd, Nonlinear Optics, Academic Press, New York, 1992.
[31] D.S. Chemla, J. Zyss (Eds.), Nonlinear Optical Properties of Organic Molecules and Crystals I, Academic Press, New York, 1987, p. 23.
[32] R.L. Sutherland, Handbook of Nonlinear Optics, Marcel Dekker, New York, 1996.
[33] D.S. Chemla, J.L. Oudar, J. Jerphagon, J. Phys. Rev. B 12 (1975) 4534.
[34] K. Clays, A. Persoons, Rev. Sci. Instrum. 63 (1992) 3285.
[35] M. Sheik-Bahae, A.A. Said, T. Wei, D.J. Hagan, E.W. van Stryland, IEEE J. Quantum Electron. 26 (1990) 760.
[36] S. Di Bella, M.A. Ratner, T.J. Marks, J. Am. Chem. Soc. 114 (1992) 5842.
[37] S. Di Bella, T.J. Marks, M.A. Ratner, J. Am. Chem. Soc. 116 (1994) 4440.

[38] J.L. Oudar, J. Chem. Phys. 67 (1977) 446.
[39] J.L. Oudar, R.J. Hierle, J. Appl. Phys. 48 (1977) 2699.
[40] R.H. Naulty, M.P. Cifuentes, M.G. Humphrey, S. Houbrechts, C. Boutton, A. Persoons, G.A. Heath, D.C.R. Hockless, B. Luther-Davies, M. Samoc, J. Chem. Soc., Dalton Trans. (1997) 4167.
[41] R.H. Naulty, A.M. McDonagh, I.R. Whittall, M.P. Cifuentes, M.G. Humphrey, S. Houbrechts, J. Maes, A. Persoons, G.A. Heath, D.C.R. Hockless, J. Organomet. Chem. 563 (1998) 137.
[42] V. Cadierno, S. Conejero, M.P. Gamasa, J. Gimeno, I. Asselberghs, S. Houbrechts, K. Clays, A. Persoons, J. Borge, S. Garcia-Granda, Organometallics 18 (1999) 582.
[43] I.-Y. Wu, J.T. Lin, J. Luo, C.-S. Li, C. Tsai, Y.S. Wen, C.-C. Hsu, F.-F. Yeh, L. Sean, Organometallics 17 (1998) 2188.
[44] A.M. McDonagh, M.P. Cifuentes, N.T. Lucas, M.G. Humphrey, S. Houbrechts, A. Persoons, J. Organomet. Chem. 605 (2000) 184.
[45] A.M. McDonagh, N.T. Lucas, M.P. Cifuentes, M.G. Humphrey, S. Houbrechts, A. Persoons, J. Organomet. Chem. 605 (2000) 193.
[46] S. Houbrechts, K. Clays, A. Persoons, V. Cadierno, M.P. Gamasa, J. Gimeno, I.R. Whittall, M.G. Humphrey, Proc. SPIE-Int. Soc. Opt. Eng. 2852 (1996) 97.
[47] S. Houbrechts, K. Clays, A. Persoons, V. Cadierno, M.P. Gamasa, J. Gimeno, Organometallics 15 (1996) 5266.
[48] S. Hurst, M.P. Cifuentes, J.P. Morrall, N.T. Lucas, I.R. Whittall, M.G. Humphrey, I. Asselberghs, A. Persoons, M. Samoc, B. Luther-Davies, A.C. Willis, Organometallics 20 (2001) 4664.
[49] S. Hurst, N.T. Lucas, M.P. Cifuentes, M.G. Humphrey, M. Samoc, B. Luther-Davies, I. Asselberghs, R.V. Boxel, A. Persoons, J. Organomet. Chem. 633 (2001) 114.
[50] C.E. Powell, M.P. Cifuentes, A.M. McDonagh, S. Hurst, N.T. Lucas, C.D. Delfs, R. Stranger, M.G. Humphrey, S. Houbrechts, I. Asselberghs, A. Persoons, D.C.R. Hockless, Inorg. Chim. Acta 352 (2003) 9.
[51] I.R. Whittall, M.G. Humphrey, A. Persoons, S. Houbrechts, Organometallics 15 (1996) 1935.
[52] T. Weyland, I. Ledoux, S. Brasselet, J. Zyss, C. Lapinte, Organometallics 19 (2000) 5235.
[53] A.M. McDonagh, M.G. Humphrey, M. Samoc, B. Luther-Davies, S. Houbrechts, T. Wada, H. Sasabe, A. Persoons, J. Am. Chem. Soc. 121 (1999) 1405.
[54] S. Hurst, M.G. Humphrey, T. Isoshima, K. Wostyn, I. Asselberghs, K. Clays, A. Persoons, M. Samoc, B. Luther-Davies, Organometallics 21 (2002) 2024.
[55] A.M. McDonagh, M.P. Cifuentes, M.G. Humphrey, S. Houbrechts, J. Maes, A. Persoons, M. Samoc, B. Luther-Davies, J. Organomet. Chem. 610 (2000) 71.
[56] I.R. Whittall, M.P. Cifuentes, M.G. Humphrey, B. Luther-Davies, M. Samoc, S. Houbrechts, A. Persoons, G.A. Heath, D.C.R. Hockless, J. Organomet. Chem. 549 (1997) 127.
[57] I.-Y. Wu, J.T. Lin, J. Luo, S.-S. Sun, C.-S. Li, K.J. Lin, C. Tsai, C.-C. Hsu, J.-L. Lin, Organometallics 16 (1997) 2038.
[58] I.R. Whittall, M.G. Humphrey, S. Houbrechts, J. Maes, A. Persoons, S. Schmid, D.C.R. Hockless, J. Organomet. Chem. 544 (1997) 277.
[59] S. Hurst, N.T. Lucas, M.G. Humphrey, I. Asselberghs, R.V. Boxel, A. Persoons, Aust. J. Chem. 54 (2001) 447.
[60] I.R. Whittall, M.P. Cifuentes, M.G. Humphrey, B. Luther-Davies, M. Samoc, S. Houbrechts, A. Persoons, G.A. Heath, D. Bogsányi, Organometallics 16 (1997) 2631.
[61] I.R. Whittall, M.G. Humphrey, S. Houbrechts, A. Persoons, D.C.R. Hockless, Organometallics 15 (1996) 5738.
[62] S.K. Hurst, M.P. Cifuentes, A.M. McDonagh, M.G. Humphrey, M. Samoc, B. Luther-Davies, I. Asselberghs, A. Persoons, J. Organomet. Chem. 642 (2002) 259.
[63] M.P. Cifuentes, J. Driver, M.G. Humphrey, I. Asselberghs, A. Persoons, M. Samoc, B. Luther-Davies, J. Organomet. Chem. 607 (2000) 72.
[64] S.R. Marder, J.W. Perry, W.P. Schaefer, B.G. Tiemann, Proc. SPIE-Int. Soc. Opt. Eng. 1147 (1989) 108.
[65] I.R. Whittall, M.P. Cifuentes, M.J. Costigan, M.G. Humphrey, S.C. Goh, B.W. Skelton, A.H. White, J. Organomet. Chem. 471 (1994) 193.
[66] I.R. Whittall, M.G. Humphrey, M. Samoc, B. Luther-Davies, D.C.R. Hockless, J. Organomet. Chem. 544 (1997) 189.
[67] I.R. Whittall, M.G. Humphrey, D.C.R. Hockless, B.W. Skelton, A.H. White, Organometallics 14 (1995) 3970.
[68] A.M. McDonagh, I.R. Whittall, M.G. Humphrey, B.W. Skelton, A.H. White, J. Organomet. Chem. 519 (1996) 229.
[69] A.M. McDonagh, I.R. Whittall, M.G. Humphrey, D.C.R. Hockless, B.W. Skelton, A.H. White, J. Organomet. Chem. 523 (1996) 33.
[70] L.K. Myers, C. Langhoff, M.E. Thompson, J. Am. Chem. Soc. 114 (1992) 7560.
[71] M.E. Thompson, W. Chiang, L.K. Myers, C. Langhoff, Proc. SPIE-Int. Soc. Opt. Eng. 1497 (1991) 423.
[72] L.K. Myers, D.M. Ho, M.E. Thompson, C. Langhoff, Polyhedron 14 (1995) 57.
[73] I.R. Whittall, M.G. Humphrey, M. Samoc, J. Swiatkiewicz, B. Luther-Davies, Organometallics 14 (1995) 5493.
[74] A.M. McDonagh, M.G. Humphrey, M. Samoc, B. Luther-Davies, Organometallics 18 (1999) 5195.
[75] A.M. McDonagh, M.P. Cifuentes, I.R. Whittall, M.G. Humphrey, M. Samoc, B. Luther-Davies, D.C.R. Hockless, J. Organomet. Chem. 526 (1996) 99.
[76] S.K. Hurst, N.T. Lucas, M.G. Humphrey, T. Isoshima, K. Wostyn, I. Asselberghs, K. Clays, A. Persoons, M. Samoc, B. Luther-Davies, Inorg. Chim. Acta 350 (2003) 62.
[77] S.K. Hurst, M.G. Humphrey, J.P. Morrall, M.P. Cifuentes, M. Samoc, B. Luther-Davies, G.A. Heath, A.C. Willis, J. Organomet. Chem. 670 (2003) 56.
[78] C.C. Frazier, E.A. Chauchard, M.P. Cockerham, P.L. Porter, Mater. Res. Soc. Symp. Proc. 109 (1988) 323.
[79] P.L. Porter, S. Guha, K. Kang, C.C. Frazier, Polymer 32 (1991) 1756.
[80] W.J. Blau, H.J. Byrne, D.J. Cardin, A.P. Davey, J. Mater. Chem. 1 (1991) 245.
[81] A.P. Davey, D.J. Cardin, H.J. Byrne, W.J. Blau (Eds.), Organic Molecules for Nonlinear Optics and Photonics, Kluwer Academic Publishers, Dordrecht, 1991, p. 391.
[82] A.P. Davey, H. Page, W.J. Blau, Synth. Met. 55–57 (1993) 3980.
[83] J. Haub, M. Johnson, B. Orr, M. Woodruff, G. Crisp, Presented at CLEO/QUELS, Baltimore, 1991.
[84] S. Guha, K. Kang, P.L. Porter, J.F. Roach, D.E. Remy, F.J. Aranda, D.V.G. Rao, Opt. Lett. 17 (1992) 264.
[85] S. Guha, C.C. Frazier, W.P. Chen, P.L. Porter, K. Kang, Proc. SPIE-Int. Soc. Opt. Eng. 1105 (1989) 14.
[86] H. Page, W.J. Blau, A.P. Davey, X. Lou, D.J. Cardin, Synth. Met. 63 (1994) 179.
[87] C.C. Frazier, S. Guha, W.P. Chen, M.P. Cockerham, P.L. Porter, C.H. Lee, Polymer 28 (1987) 553.
[88] S. Guha, C.C. Frazier, P.L. Porter, K. Kang, S.E. Finberg, Opt. Lett. 14 (1989) 952.
[89] I.R. Whittall, M.G. Humphrey, M. Samoc, B. Luther-Davies, Angew. Chem. Int. Ed. Engl. 36 (1997) 370.
[90] J. Vicente, M.T. Chicote, M.D. Abrisqueta, M.C. Ramirez de Arellano, M.G. Humphrey, M.P. Cifuentes, M. Samoc, B. Luther-Davies, Organometallics 19 (2000) 2968.
[91] B.K. Teo, Y.H. Xu, B.Y. Zhong, Y.K. He, H.Y. Chen, W. Qian, Y.J. Deng, Y.H. Zou, Inorg. Chem. 40 (2001) 6794.
[92] B.J. Coe, Chem. Eur. J. 5 (1999) 2464.
[93] M.P. Cifuentes, C.E. Powell, M.G. Humphrey, G.A. Heath, M. Samoc, B. Luther-Davies, J. Phys. Chem. A 105 (2001) 9625.
[94] C.E. Powell, M.P. Cifuentes, J.P. Morrall, R. Stranger, M.G. Humphrey, M. Samoc, B. Luther-Davies, G.A. Heath, J. Am. Chem. Soc. 125 (2003) 602.
[95] M.H. Garcia, M.P. Robalo, A.R. Dias, M.T. Duarte, W. Wenseleers, G. Aerts, E. Goovaerts, M.P. Cifuentes, S. Hurst, M.G. Humphrey, M. Samoc, B. Luther-Davies, Organometallics 21 (2002) 2107.